



Diversity in times of adversity: probabilistic strategies in microbial survival games

Denise M. Wolf^{a,*}, Vijay V. Vazirani^b, Adam P. Arkin^c

^aPhysical Biosciences Division, Lawrence Berkeley National Laboratory, 1 Cyclotron Road, Berkeley, CA 94720, USA

^bCollege of Computing, Georgia Institute of Technology, Atlanta, GA 30332-0280, USA

^cHoward Hughes Medical Institute, Department of Bioengineering, University of California; Physical Biosciences Division, Lawrence Berkeley National Laboratory, 1 Cyclotron Road, MS 3-144, Berkeley, CA 94720, USA

Received 3 August 2004; received in revised form 4 November 2004; accepted 18 November 2004

Abstract

Population diversification strategies are ubiquitous among microbes, encompassing random phase-variation (*RPV*) of pathogenic bacteria, viral latency as observed in some bacteriophage and HIV, and the non-genetic diversity of bacterial stress responses. Precise conditions under which these diversification strategies confer an advantage have not been well defined. We develop a model of population growth conditioned on dynamical environmental and cellular states. Transitions among cellular states, in turn, may be biased by possibly noisy readings of the environment from cellular sensors. For various types of environmental dynamics and cellular sensor capability, we apply game-theoretic analysis to derive the evolutionarily stable strategy (*ESS*) for an organism and determine when that strategy is diversification. We find that: (1) *RPV*, effecting a sort of Parrondo paradox wherein random alternations between losing strategies produce a winning strategy, is selected when transitions between different selective environments cannot be sensed, (2) optimal *RPV* cell switching rates are a function of environmental lifecycle asymmetries and environmental autocorrelation, (3) probabilistic diversification upon entering a new environment is selected when sensors can detect environmental transitions but have poor precision in identifying new environments, and (4) in the presence of excess additive noise, low-pass filtering is required for evolutionary stability. We show that even when *RPV* is not the *ESS*, it may minimize growth rate variance and the risk of extinction due to ‘unlucky’ environmental dynamics.

© 2005 Elsevier Ltd. All rights reserved.

Keywords: Random phase variation; Game theory; Stochastic; Bacteria; Sensors

1. Introduction

“Adversity has the effect of eliciting talents, which in prosperous circumstances would have lain dormant.”—Horace (65BC–6BC)

Why do some bacterial environmental responses blink on and off like Christmas lights while others respond definitively or in graded fashion to environmental and cellular signals? Examples of these ‘blinking’, or phase

variable phenotypes include type I and IV pilus varieties in uropathic *Escherichia coli*, *Neisseria gonorrhoeae*, and *Neisseria meningitidis* (Abraham et al., 1985; Howell–Adams and Seifert, 2000; Power et al., 2003); toxin production, fimbriae, lipopolysaccharide variants, and restriction-modification genes in *Mycobacterium pulmonis* (Dybvig et al., 1998); outer membrane proteins in *Dichelobacter nodosus* (Moses et al., 1995); flagellum in *Salmonella typhimurium* (Bonifield and Hughes, 2003); phage growth limitation machinery in *Streptomyces coelicolor* (Sumbly and Smith, 2003); and many others (Henderson et al., 1999; Hallet, 2001).

The machinery that implements phase variation is diverse, providing an intriguing example of convergent

*Corresponding author. Tel.: +510 495 2366; fax: +510 486 6059.

E-mail addresses: dmwolf@lbl.gov (D.M. Wolf), vazirani@cc.gatech.edu (V.V. Vazirani), aparkin@lbl.gov (A.P. Arkin).

evolution. Phase variation mechanisms involving reversible genetic changes in specific genomic loci include slipped-strand mispairing mechanisms, site-specific DNA rearrangements, and DNA shuffling by gene conversion and allele replacement (Hallet, 2001). Other population diversification mechanisms, such as the methylation-based switch controlling pyelonephritis-associated pilus (*pap*) expression in *E. coli* (Blomfield, 2001; Hernday et al., 2002), and the genetic reaction networks controlling competence for DNA transformation, sporulation, and a myriad of alternative metabolic pathways in *Bacillus subtilis* (Grossman, 1995; Msadek, 1999), are epigenetic in nature. A particularly fascinating example is the partitioning of *Streptococcus pneumoniae* populations into lysing ‘donor’ and DNA uptake ‘recipient’ subpopulations, the control of which is achieved epigenetically by the ComCDE signal transduction pathway (Steinmoen et al., 2002).

Observations of population diversification open up a number of fundamental questions about the origin and purpose of phenotypic noise. The most basic of these questions is whether this noise is controlled or incidental: evolutionarily advantageous, deleterious, or neutral? If stress response diversification is indeed controlled and selected for rather than incidental, this sets the stage for three lines of inquiry, essentially the ‘what’, ‘how’, and ‘why’ of diversification. The first (what) is the quantification of stress response diversification in a microbe. Though microbiologists have measured phenotypic response heterogeneity of individual developmental and virulence-associated pathways, for example sporulation and competence for transformation in *B. subtilis* (Grossman, 1995) and the environmental modulation of type 1 piliation rates in uropathic *E. coli* (Gally et al., 1993), there have been few systematic efforts to quantify how microbes map a sensed environment into a plurality of cellular phenotypes. A second line of inquiry (how) elucidates the causal basis for diversification. Still unclear is how environmental signals are transduced to modulate heterogeneity; the role of pathway ‘cross-talk’ in coordinating stress phenotypes; the function, if any, of different phase variation mechanisms; and how non-phase variable, epigenetic diversification like that found in the soil growing microbe *B. subtilis* is achieved. A third line of inquiry, the focus of this paper and its companion (Wolf et al., 2005), is on the ‘whys’ of diversification. Why do bacteria diversify? What are the evolutionary origins and fitness consequences of diversification?

Control systems, whether human engineered or biological, balance performance trade-offs between controllability and sensitivity. A regulatory network can be tightly controlled, producing a deterministic, noise-filtered outcome, but it does so at the cost of reduced sensitivity to small fluctuations in input signals. Conversely, such a network can be configured to be highly sensitive to small fluctuations in input signals, but

this sensitivity exacts a cost in the form of noise sensitivity, which can introduce non-determinism and generate heterogeneous responses over a population (Boyd, 1991; Vidyasagar, 1992). Though it is possible that some population heterogeneity is incidental, present only because there is no strong selective pressure for homogeneity and because trade-offs between process sensitivity and controllability can be resolved in favor of sensitivity without a loss in fitness, a growing body of evidence suggests that this is not generally the case. Diversification phenotypes among pathogenic bacteria are believed to aid survival within a host by allowing bacteria to evade the immune system or search a host’s receptor space (Henderson et al., 1999; Hallet, 2001). Evasion of the host immune system is thought to be facilitated by molecular mimicry of host structures by phase-variable lipopolysaccharides (LPS) in *Helicobacter pylori* and *Campylobacter* (Moran and Prendergast, 2001), and by the astounding level of antigenic diversity produced by 10^7 different pilus varieties in *N. gonorrhoeae* (used for host attachment and the uptake of exogenous DNA (Fussenegger et al., 1997)), whereas phase-variable *opa* genes in *Neisseria* are believed to orchestrate the recognition of different host receptors and result in tissue tropism (Hauck and Meyer, 2003). Phase variation between a small number of phenotypes (e.g. type 1 pili expression) does not fit neatly into these categories, and for the most part, the experiments and theory needed to test these hypotheses have yet to be done. Those that have been performed, such as the *bvgAS* knockout and phase-lock experiments in *Bordetella* strains showing that *RPV* of *bvgS* is not required for virulence, but that a Bvg^- phenotype is necessary for growth outside a host (Weiss and Falkow, 1984; Stibitz et al., 1989; Martinez de Tejada et al., 1998; Coote, 2001), hint at a more complex story than these folk theories can account for.

Phenotypic diversification has also been hypothesized to be a form of bet hedging, a survival strategy analogous to stock market portfolio management. From this point of view, ‘selfish’ genotypes diversify assets among multiple stocks (phenotypes) to minimize the long-term risk of extinction and maximize the long-term expected growth rate in the presence of (environmental) uncertainty. Stochastic parsing of viral populations into lytic and lysogenic (or latent) states, for example, is believed to have evolved as an adaptive solution to fluctuations in the availability of bacterial hosts (Mittler, 1996; Stumpf et al., 2002). Dispersal phenotypes could be subject to bet hedging as well; when an environment consists of niches that become available stochastically for colonization, the optimal genotype produces a mix of dispersing and non-dispersing progeny (Comins et al., 1980). Bet hedging in the plant kingdom might also be common, as exemplified by the probabilistic germination strategies favored by desert plants subjected to

random rain-drought patterns (Satake et al., 2001). Further evidence for this view of microbes as single-celled stockbrokers might be found in observations that stress phenotypes introduce a trade-off between a fitness advantage under stress with a fitness defect under more favorable conditions (Cooper and Lenski, 2000; Kishony and Leibler, 2003). Diversification could be a response to this trade-off ensuring the availability of ‘favoured’ phenotypes for growth in each environmental condition.

In this paper and its short companion paper (Wolf et al., 2005) we use evolutionary game theory to formally explore the origin and utility of random phase variation (*RPV*). Though *in silico* theories cannot in themselves definitively explain the genesis and utility of any particular phase varying phenotype—experiments are needed for that—an evolutionarily game theoretic treatment can help uncover general principles at work in canalizing evolution toward phase varying expression patterns, and could provide an intellectual framework from which to design and interpret experiments. Our game theoretic formulation posits bacteria as players in a game of survival pitting cell against cell, and cell against nature. Each cell has a number of moves it can play in this game. Moves available to cells are cell states or phenotypes. The number of ‘moves’ in this game can be few—e.g. pili expression that can be on or off—or many, for example if different kinds of fimbriae, surface receptors, hemolysins, toxins, type IV fimbriae, type III secretion apparatus and other pathways can be turned on and off in different combinations at different times. Cells may have sensors that enable them to sense the environment, and possibly intercellular signals like quorum sensing peptides as well. These sensors can be noisy, providing false or misleading information about the environment. A strategy in this game of survival is a map from sensor information onto behaviour. A strategy is called evolutionarily stable (ESS) if a population of cells adopting this strategy cannot be invaded by a mutant adopting a different strategy over the same set of ‘moves’, or phenotypes. Thus, a game theoretic analysis of cellular behaviour, for example *RPV*, looks at behavior as the ESS strategy in a game of survival. The question then becomes, what was/is the problem, if this behaviour is the solution? What types of environments and—because we are interested in the role of information in determining the ESS—sensing capacity select for *RPV* or other diversification strategies? Alternatively, given a lifestyle and a set of phenotypes, what is the best expression strategy? How should phenotypes be deployed in order to minimize the risk of extinction?

As shown in this paper and in (Wolf et al., 2005), evolutionarily stable phenotype expression strategies depend strongly on the selective forces over the *entire lifecycle* of the organism, in conjunction with the ability

of the organism to *sense* its environment. By lifecycle we refer to all the environmental conditions that an organism might find itself in—inside a host, outside a host, in different host compartments, in different external environments—and the expected order and amount of time spent in each. In the sections below we look at different types of sensor defects (unobservable environmental transitions, incorrect identification of environmental states, signal transduction delays, and additive noise), and different classes of environments (time-invariant, time-varying and stochastic), and analyse for combinations that give rise to *RPV* as an ESS. Frequency-dependent environments are considered in (Wolf et al., 2005). For those combinations that do not select for *RPV*, we analyse for the ‘alternative’ ESS. As demonstrated in the sections that follow, a strategy that is evolutionarily stable under one set of environmental and sensing conditions can be impossible to implement or lead to extinction in other circumstances. Moreover, microbial populations with different sensor profiles in the exact same environment(s) will adopt different evolutionarily stable strategies depending on the types of sensing failures they experience.

2. The microbial diversification game (MDG) model

Our model defines the state of a cell to be the combined (discrete) expression states of a finite number of cellular programs (e.g. type 1 pili = ON, flagellar motility = OFF, toxin synthesis = ON). Cells live potentially complex lifestyles (in and out of hosts, in water or dirt, in different cellular compartments, in fluctuating pH, osmolarity, nutrient composition, and so on), which we represent by a Markov process over a finite number of environmental states E_i . The cells may be equipped with environmental sensors $q = (\Delta E, \bar{E})$ providing (noisy) estimates of environmental state (\bar{E}) and the likelihood that an environmental transition has occurred in the last increment of time (ΔE). A cell’s overall *lifecycle strategy* \mathcal{S} is a map from environmental sensor data q to cellular behavior probability, represented in our model in terms of *sub-strategies* S_i defined by Markov chains over cellular state space ($\mathcal{S}: q \mapsto S_i$). Thus, a cell’s lifecycle strategy directs cellular behavior probability on the basis of information gathered from its sensors, effectively tracing a sensor-modulated stochastic trajectory through the cellular state space defining its physiology.

Specifically, our general model captures (1) time-invariant, deterministically or stochastically time-varying, or frequency dependent environments, (2) environmental sensors with a range of sensor defects including unobservable environmental transitions, incorrect identification of environmental states, signal transduction delays, and additive noise, and (3) four classes of

Table 1
Strategies representable by the MDG model

| Strategy | Example | Parameter constraints |
|-------------------------------------|--|---|
| Sensor-independent pure | Express pili | $sx_1 = 0; sy_1 > 0; sx_2 = 0; sy_2 > 0;$ $P_1 = 1; P_2 = 0$ |
| Sensor-based pure | IF the sensor reads environment $E1$, express pili; ELSE, do not | $sx_1 = 0; sy_1 > K_f^b; sx_2 > K_f; sy_2 = 0;$ $P_1 = 1; P_2 = 0$ |
| Sensor-based pure; LPF ^a | IF the sensor reads environment $E1$, express pili; ELSE, do not. Low pass filter the sensor signal | $sx_1 = 0; K_f \gg sy_1 > 0; K_f \gg sx_2 > 0;$ $sy_2 = 0; P_1 = 1; P_2 = 0$ |
| Sensor-based mixed | IF the sensor reads $E1$, express pili with probability $P_1(0 < P_1 < 1)$ | $sx_1 = 0; sy_1 > K_f; sx_2 > K_f; sy_2 = 0;$ $P_1 < 1; P_2 > 0.$ |
| Sensor-based mixed; LPF | IF the sensor reads $E1$, express pili with probability $P_1(0 < P_1 < 1)$. Low-pass filter the sensor input signal | $sx_1 = 0; K_f \gg sy_1 > 0;$ $K_f \gg sx_2 > 0; sy_2 = 0; P_1 < 1; P_2 > 0$ |
| Random phase variation (RPV) | IF the sensor reads Ei , randomly alternate between pilated and unpilated states at rates (sx_i, sy_i) | $sx_1 > 0; sy_1 > 0; sx_2 > 0; sy_2 > 0;$ $P_1 = 1; P_2 = 0$ |

^aLPF = low-pass filtered.

^b K_f is a fast switching rate, ≈ 3 – 20 for the other parameters used in this paper.

Table 2
Environmental sensor defects representable by the MDG model

| Sensor feature | Categories and parameter regimes |
|---|---|
| Observability (O) (environmental transitions) | Perfect ($pObs = 1$); none ($pObs = 0$); imperfect ($0 < pObs < 1$) |
| Accuracy (A) (identifying environments) | Perfect ($Ps_{ij} = 1, Ps_{ij} = 0; i \neq j$); none ($Ps_{ij} = 0.5$); imperfect ($Ps_{ii} < 1$ or $0 < Ps_{ij} : i \neq j$) |
| Additive noise (N) | None ($rate = 0$); high ($rate > K_n^a$); some ($0 < rate < K_n$) $sq_{i,j} = rate/2$ |
| Delays (D) | Short ($sx + sy \gg \varepsilon^b$); long ($sx + sy < \varepsilon$) |
| Sampling frequency (informative noise) | None ($rate = 0$); high ($rate > K_n$); medium ($0 < rate < K_n$). $sq_{2,1}(1) = rate/(1 + r1); sq_{1,2}(1) = r1 \times sq_{1,2}(1); sq_{1,2}(2) = rate/(1 + r2); sq_{2,1}(2) = r2 \times sq_{1,2}(2); r1 = pObsPs_{21}/Ps_{11} + (1 - pObs); r2 = pObsPs_{12}/Ps_{22} + (1 - pObs)$ |

^a K_n is a high level of noisy sensor-state switching, ≈ 1 – 20 for the other parameters used in this paper.

^b ε is a slow cell-state switching rate, in effect implementing a signal transduction delay (≈ 0.1 for the other parameters used in this paper).

formulation that contributes to the model's ability to represent different levels of sensor accuracy, additive noise, and signal processing delays (see Table 2).

Next we introduce the environmental transition matrices T_{ji} . These matrices permit representation of sensor-based mixed strategies, and explicitly capture the ability of a sensor to observe environmental transitions, a probability that is decoupled from the sensor's accuracy in identifying a new environment should a transition be observed. If the environment is time varying, then at each time step k , the environment can either stay the same as it was at the previous time step, or transition to a new environmental state. If the environment does not change at time step k ($E(k) = E(k-1) = Ei$), then the environmental transition matrix T_{ii} is the identity matrix $I_{4 \times 4}$ (1's along the diagonal, 0 at off-diagonals). In this case, the population vector is updated according to the map $\vec{X}_{k+1} = R_{di}(k)\vec{X}_k$ (Eq. (1) with $T_{ji} = I_{4 \times 4}$). If, however, the environment does change at time step k , transitioning from Ej to Ei , $i \neq j$, T_{ji} is given by the matrix $T_{12} = [(1 - p_{Obs12})I + p_{Obs12}MS_1]$ if the environment transi-

tions from state $E1$ to $E2$, and by $T_{21} = [(1 - p_{Obs21})I + p_{Obs21}MS_2]$ if the environment transitions from state $E2$ to $E1$. These transition matrices are functions of (1) the parameter $p_{Obsji} \in [0, 1]$, the probability that an environmental state transition from Ej to Ei is observed by a cell, and (2) sensor accuracy matrices S_i , where

$$S_i = \begin{bmatrix} Ps_{1i} & 0 & Ps_{1i} & 0 \\ 0 & Ps_{1i} & 0 & Ps_{1i} \\ Ps_{2i} & 0 & Ps_{2i} & 0 \\ 0 & Ps_{2i} & 0 & Ps_{2i} \end{bmatrix} \quad (3)$$

and the non-zero matrix entries Ps_{ij} are the probabilities that the environmental sensor reads $\vec{E} = Ei$ after the environment changes to $\vec{E} = Ej$ should a transition be observed. The rows of the sensor accuracy matrix S_i take the fraction of the population that observed an environmental transition (p_{Obsji}) and repartition it according to the ability of the sensors to accurately identify a new environmental state. If, for example, the sensor is perfect, all cells observe an environmental transition should it occur ($p_{Obsji} = 1$), and all cells

correctly identify the new environmental state ($P_{s_{ij}} = 1$ if $i = j$, and $P_{s_{ij}} = 0$ if $i \neq j$).

Transition matrices T_{ji} are also functions of a strategy mixing matrix M , where

$$M = \begin{bmatrix} P_1 & 0 & P_2 & 0 \\ 0 & P_1 & 0 & P_2 \\ 1 - P_1 & 0 & 1 - P_2 & 0 \\ 0 & 1 - P_1 & 0 & 1 - P_2 \end{bmatrix} \quad (4)$$

and P_i , $i = 1, 2$, are the probabilities defining mixed strategies (i.e. if the sensor registers an environmental transition, and the estimate of the new environmental state is $\vec{E} = E_i$, pick sub-strategy S_1 (defined by s_{x_1} and s_{y_1}) with probability P_i and sub-strategy S_2 (defined by s_{x_2} and s_{y_2}) with probability $(1 - P_i)$). The first column of M partitions the subpopulation of cells in state x with sensors reading $\vec{E} = E_1$ (implementing sub-strategy S_1) into fractions, with P_1 of the cells retaining the x cell state and S_1 sub-strategy, and $1 - P_1$ of the cells retaining the x cell state but shifting to the S_2 sub-strategy. If, for example, S_1 is the pure strategy of all cells being in the x -state ($s_{x_1} = 0$ and $s_{y_1} > 0$), and S_2 is the pure strategy of all cells being in the y -state ($s_{x_2} > 0$ and $s_{y_2} = 0$), then an application of M with $P_1 < 1$ has the effect of probabilistically diversifying the population into x and y subpopulations upon sensing an environmental transition.

Fig. 1 summarizes the model of Eq. (1). In short, if the environment does not change at time $k\Delta t$, the population vector \vec{X} is updated according to the rate matrix R_i , which captures cell birth, death, cell state switching, and sensor dynamics. If the environment does change state

at time $k\Delta t$, the observability parameter $p_{Obs_{ji}}$ partitions the population into those cells that observe the transition ($p_{Obs_{ji}}\vec{X}$) and those that do not ($(1 - p_{Obs_{ji}})\vec{X}$). Of the cells that do observe a transition, the accuracy matrix S_i further partitions the subpopulation into those cells that correctly determine the new environmental state, and those that do not. If the population uses a mixing strategy, the subpopulation that observed the environmental transition is further partitioned probabilistically by the mixing matrix M into subpopulations adopting sub-strategies S_1 (defined by s_{x_1} and s_{y_1}) and S_2 (s_{x_2}, s_{y_2}). Following these successive partitions, the rate matrix R_i is applied to capture cell birth and death, and to complete the implementation of the sensor dynamics and the pure, sensor-based pure, sensor-based mixed, or RPV strategy employed by the population to survive. Tables 1 and 2 provide the constraints on the strategy parameters $S = (s_{x_1}, s_{y_1}, s_{x_2}, s_{y_2}, P_1, P_2)$ and the sensor profile parameters $Q = (p_{Obs_{ij}}, P_{s_{ij}}, sq_{i,j}(k))$; $i, j, k = 1 : 2$; that enable the model to represent a variety of pure, mixed, or random phase varying strategies, and the entire range of environmental sensor defects.

If the environment is time varying and stochastic, the environmental state $E(k)$ is governed by the Markov chain

$$\begin{bmatrix} PE_1(k+1) \\ PE_2(k+1) \end{bmatrix} = \begin{bmatrix} 1 - p_{1,2} & p_{2,1} \\ p_{1,2} & 1 - p_{2,1} \end{bmatrix} \begin{bmatrix} PE_1(k) \\ PE_2(k) \end{bmatrix}, \quad (5)$$

where $PE_i(k)$ is the probability of the environment being in state E_i at time $k\Delta t$ and $p_{i,j}$ is the probability of an E_i to E_j transition over one time step (Fig. 1b). The

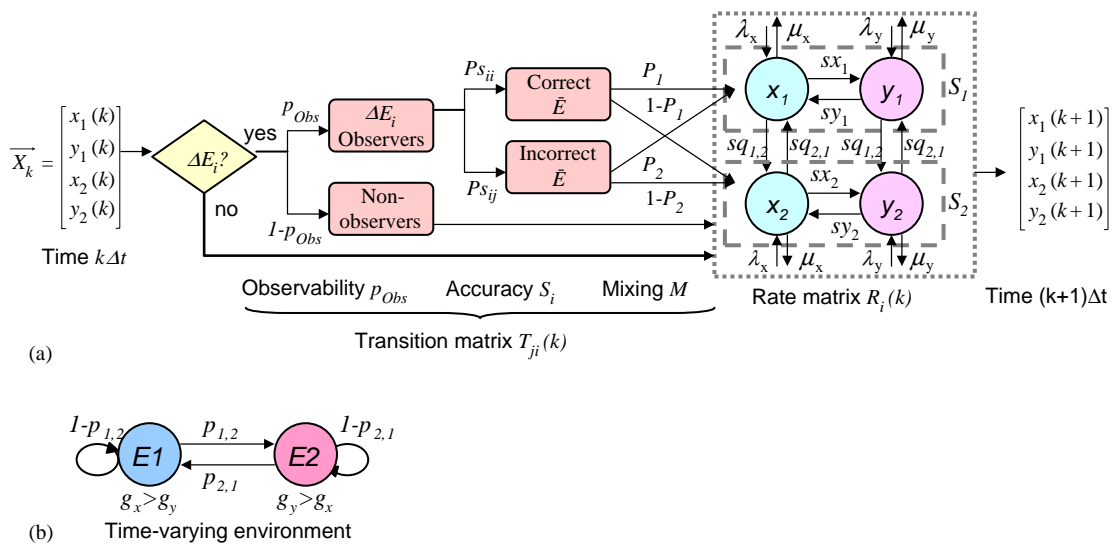


Fig. 1. Schematic representations of the microbial diversification game (MDG) model of Eq. (1) (a), and the stochastically time-varying environment of Eq. (5) (b). The mathematical details of the model are discussed in the text. The diagram in (a) shows all the factors that impact the growth and composition of a population of cells, including (imperfect) environmental sensing, phenotype expression and diversification, and environmental- and cell state- dependent growth rates.

stationary distribution over environmental states is $(\pi_1, \pi_2) = (p_{2,1}/(p_{1,2}+p_{2,1}), p_{1,2}/(p_{1,2}+p_{2,1}))$. In this case, Eqs. (1) and (5) are simulated together, with Eq. (5) producing a string of environmental states $E(1), E(2), \dots, E(k)$, which key into environmentally dependent matrices R_{di} and T_{ji} in Eq. (1) to compute the associated population growth and composition trajectory. Alternatively, deterministic, periodic environmental variation is easily implemented, as are non-Markov environmental state distributions. For a detailed description of the simulation algorithms and the parameter ranges used, see the Materials and methods section.

Evolutionarily stable strategy (ESS): In (Maynard Smith, 1973), Maynard Smith defines an evolutionarily stable strategy to be one that is uninvadable by a rare mutant with access to same set of game ‘moves’, or cellular states (all bets are off if mutants have new competing or predatory cell states—a scenario that falls outside the scope of classical evolutionary game theory). Within this framework, strategy I is an ESS if, for all $J \neq I, W(J, I) < W(I, I)$, where $W(A, B)$ is the fitness of a single A strategist in a population of B strategists, or if $W(J, I) = W(I, I)$ and, for small q , $W(J, P_{q,I,I}) < W(I, P_{q,J,I})$, where $W(I, P_{q,J,I})$ is the fitness of a J strategist in a population P consisting of $qJ + (1 - q)I$ (Maynard Smith, 1982). The latter condition defines the ESS as a mixture of J and I . If the lifecycle is deterministic and the population equations are linear, then the fitness of a strategy is given by the Malthusian exponent (maximum eigenvalue) of the population equations (Caswell, 2001). For example, cells with two possible cellular states x and y living in a periodically time-varying environment that alternates between spending N_1 generations in environmental state E_1 and N_2 generations in E_2 , the ESS (if unique) is that strategy $S = (sx_1, sy_1, sx_2, sy_2, P_1, P_2)$ maximizing $\alpha_S = \max(\text{eig}([T_{21}R_{d2}^{N_2}T_{12}R_{d1}^{N_1}]))$, given the cell- and environmental-state-dependent cell growth rates $\lambda_x(i)$, $\mu_x(i)$, $\lambda_y(i)$, and $\mu_y(i)$, $i = 1 : 2$, and the sensor profile of the population $Q = (p_{Obsj}, P_{Sij}, sq_{ij}(k))$, $i, j, k = 1:2$ (used in Sections 3.1 and 3.2).

The Lyapunov exponent, $\log(\lambda_s) = \lim_{t \rightarrow \infty} \log(N(t))/t$, where $N(t) = \sum_j \bar{X}(i)$ is the number of cells in the population at time t , is often used in ESS analysis of populations inhabiting stochastically time-varying environments, a practice supported by Tuljapurkar’s proof that Strategy A can invade Strategy B with probability 1 if and only if $\log(\lambda_s)^A > \log(\lambda_s)^B$ (Tuljapurkar, 1982, 1990). However, the use of Lyapunov exponents in ESS analysis suffers from a serious drawback: it does not take quasi-extinction into account, and thus neglects the risks of extinction due to out-competition by a mutant over the short term or from ‘unlucky’ environmental trajectories. Thus we look at strategies that maximize $\log(\lambda_s)$, but also track growth rate variance σ^2 . Together

these measures provide a better measure of fitness than does $\log(\lambda_s)$ alone (e.g. (Lande and Orzack, 1988) and Section 14.8.1 in (Caswell (2001))). For details on our strategy fitness, ESS, $\log(\lambda_s)$, and σ^2 calculations, see the Materials and methods section.

3. Results

3.1. Eyes shut: phase variation without sensors in a time-varying environment

Consider a hypothetical bacterium with perfect, noiseless sensors capable of transducing environmental signals into a reliable measure of environmental state. Such a bacterium unequivocally ‘knows’ whether it is in a host or outside a host, in the bladder or in the gut, in water or in the dirt. In optimization terms, perfect sensors render the problem completely separable. Evolutionary forces can potentially craft different survival strategies for each environment in the lifecycle, and switch between them upon transition from environmental state to environmental state. If, for example, a bacterium with two possible cell states x and y (say pilated and unpiliated states) can be in one of two environmental states, E_1 or E_2 (in the host or in the dirt), and if environment E_1 selects strongly for x and strongly against y , while E_2 selects strongly against x and strongly for y , the optimal, evolutionarily stable strategy for perfect-sensing cells with no implementation cost for transition from one phenotype to another is for the entire population to be in state x while in E_1 , and in state y while in E_2 . This deterministic strategy, known in game theory as a (sensor-based) pure strategy (in situation 1, do A; in situation 2, do B) (Maynard Smith, 1982), leads to optimally unbounded growth of the population and uninvadability.

However, without environmental sensors (e.g. two-component systems), this strategy is not realizable. Without environmental sensors, the problem of finding a best phenotype expression strategy is *no longer separable* over the lifecycle of the organism. A bacterium without a sensor does not know whether it is in a host, in the dirt, in the water, or elsewhere and thus cannot adjust its expression strategy according to the demands of each particular environmental state. The strategies available to the two cell state, two environment example above are (1) the entire population in state x , (2) the entire population in state y , (3) a (statically) mixed population (i.e. a polymorphism in x and y , either genetic or the product of an infinitely long-lived, heritable, epigenetic differentiation), and (4) phase variation of individual cells between states x and y . Within phase variation is the possibility of phenotype switching that is either coupled or uncoupled to replication machinery, and with switching rate probabilities that are fixed, time varying, or themselves

probabilistic with uni-, bi-, or multi-modal distributions, though we will concentrate on the Markov model presented in the previous section.

If the entire population is in state x , the optimal solution in $E1$ but not $E2$, and $(g_{x1})^{\pi_1}(g_{x2})^{\pi_2} < 1$ (g_{xi} = growth rate (1/gen) of x cells in environment Ei ; π_i = the fraction of time the environment spends in Ei), eventually the allele will go extinct. Likewise, if the entire population is in state y , the optimal solution in $E2$ but not $E1$, and $(g_{y1})^{\pi_1}(g_{y2})^{\pi_2} < 1$ (g_{yi} = growth rate (1/gen) of y cells in environment Ei), extinction also results. Genetic polymorphisms die out as well, as $E1$ eventually kills off the y -subpopulation, and $E2$ extinguishes the x -subpopulation (for a proof that temporally fluctuating environments do not promote polymorphism, see (Gillespie, 1973)). Only strategy (4), phase variation, has the potential for promoting survival when counter-selective forces are this strong and oppositely oriented in the two environmental states (see Figs. 2, 3a,b).

RPV as a Devil's Compromise or Parrondo game: We prove that with missing environmental sensors, a stochastically or periodically *time-varying* environment can select for phase varying phenotype expression, *if* different environmental states select for different cell states, and if the environmental autocorrelation is sufficiently large. We call this scenario a Devil's Compromise, because *RPV* is not optimal in any one environmental state, yet it is required for survival over the lifecycle of the organism. Alternatively, *RPV* can be viewed as a sort of Parrondo paradox wherein random alternations between losing strategies produce a winning strategy (Harmer et al. 2001). Specifically, for large enough environmental autocorrelation ρ_E or lifecycle period T , there exist switching transition probabilities s_x and s_y (switching rates from x to y and y to x (1/gen), respectively) resulting in unbounded growth of the population, a result that holds in the more general case of m environments and n cell states, as proved in the Appendix A and formally stated below in Theorem 1.

Theorem 1. (*RPV* can promote survival in a time-varying environment).

Suppose the lifecycle of a bacterial population consists of m environmental states $E1, \dots, Em$ governed by an underlying Markov chain M which is ergodic. Let (π_1, \dots, π_m) be its stationary distribution. We will assume there is a number $p > 0$ such that the probability of the population leaving any environmental state E_j is $\leq p$ (and hence the probability of staying in E_j is $\geq 1 - p$). Let s_1, \dots, s_k be the possible cell states of individual bacteria in these environments.

Let $\varepsilon, \delta > 0$ be small constants. Let $g_{i,j}$ denote the growth rate per generation of bacteria in cell state s_i while in environment E_j . We will assume that for each cell

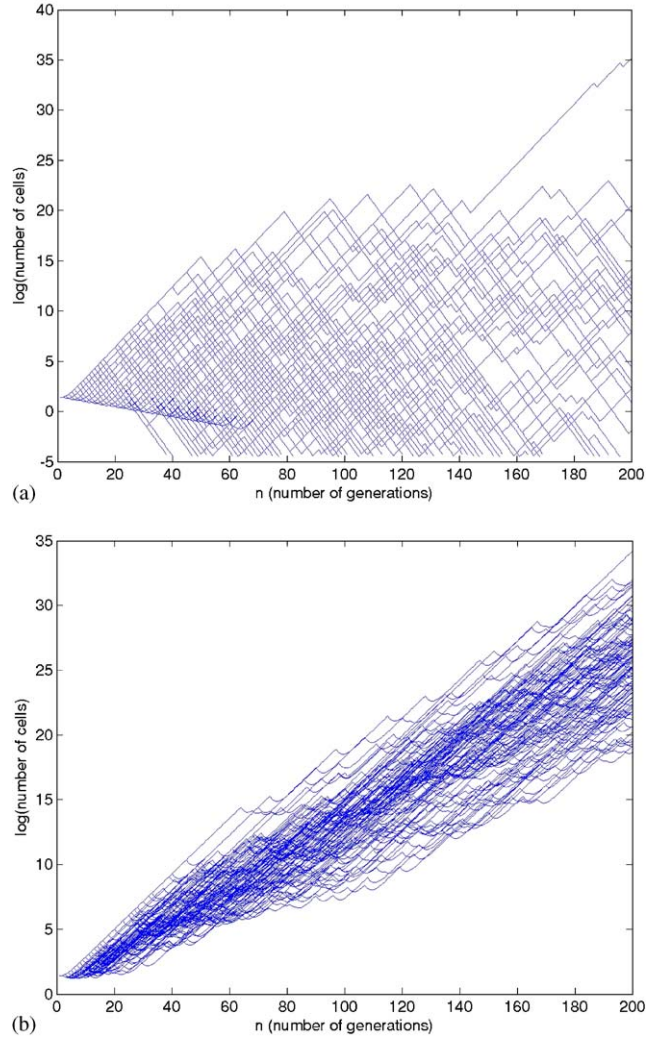


Fig. 2. *RPV* promotes survival in cells without environmental sensors living ‘Devil’s Compromise’, time-varying environments. Cells can be in two cell states, x or y , and the environment alternates between being in state $E1$ (selects for x and against y) and $E2$ (selects for y and against x) according to a Markov process with environmental transition probabilities $p_{1,2} = p_{2,1} = 0.1$ (environment alternates between spending an average 10 generations in $E1$ and $E2$). (a) Populations that are all in state x , all in state y , or a polymorphic mixture of x and y cells eventually go extinct. This plot shows 100 different trajectories starting with a polymorphic population consisting of two x cells and two y cells. (b) Populations of random phase variable cells, which alternate between being in cell states x and y ($s_x = s_y = 0.1$), can proliferate. For both plots, growth rates $\lambda_x(2) - \mu_x(2) = \lambda_y(1) - \mu_y(1) = -0.4$ and $\lambda_x(1) - \mu_x(1) = \lambda_y(2) - \mu_y(2) = 0.3$; $\Delta t = 1$.

state s_i , $\prod_{j=1}^m (g_{i,j})^{\pi_j} < 1$ (i.e. populations comprised of pure strategist cells go extinct). Further, assume that in each environment E_j , there is a cell state, denoted by $\tau(j)$, that has a positive growth rate: $g_{\tau(j),j} > 1 + 2\varepsilon$. Let

$$\lambda = \frac{2 \log((1 + 2\varepsilon)(k - 1)/\varepsilon)}{\log(1 + \varepsilon)}$$

and assume that $p \leq (1 - \delta)/\lambda$ (i.e. the environment is sufficiently autocorrelated).

Let P_2 be a population of bacteria that switch from cell state s_i to s'_i with rate α , for each pair i, i' of cell states. Though a population of bacteria that does not randomly phase vary between cell states will die out with

probability 1, there are rates of switching α such that the random phase varying population P_2 will have unbounded growth with overwhelming probability.

Proof. See Appendix A.

Optimal switching rates: *RPV* differs from a mixed strategy in classical game theory in that the strategy is defined by how often the players (cells) ‘roll their dice’ over the cell state space, as well as how these dice are weighted probabilistically. Both of these aspects of a phase variation strategy—dice weights and roll frequency—contribute to its ‘goodness’ as measured by the long-term growth rate of a population adopting the strategy. For those lifecycles giving rise to *RPV*, cell state switching rates can be too fast or too slow (Fig. 3a,b), and there are optimal switching rates that depend upon environmental lifecycle asymmetries and environmental autocorrelation ρ_E , a measure of the speed of environmental transitions (large ρ_E implies slow transition speed). Numerical experiments reveal that optimal switching rate magnitudes are inversely proportional to environmental autocorrelation (the higher the correlation, the slower the switching rates—Fig. 4b), whereas optimal switching rate asymmetries mirror lifecycle asymmetries (Fig. 4a).

These observations can be largely understood in terms of a trade-off introduced by *RPV* between the convergence rate to the steady state composition of the population (fraction of cells in each cell state), and the ‘goodness’ of this steady state (Fig. 3c). Very fast

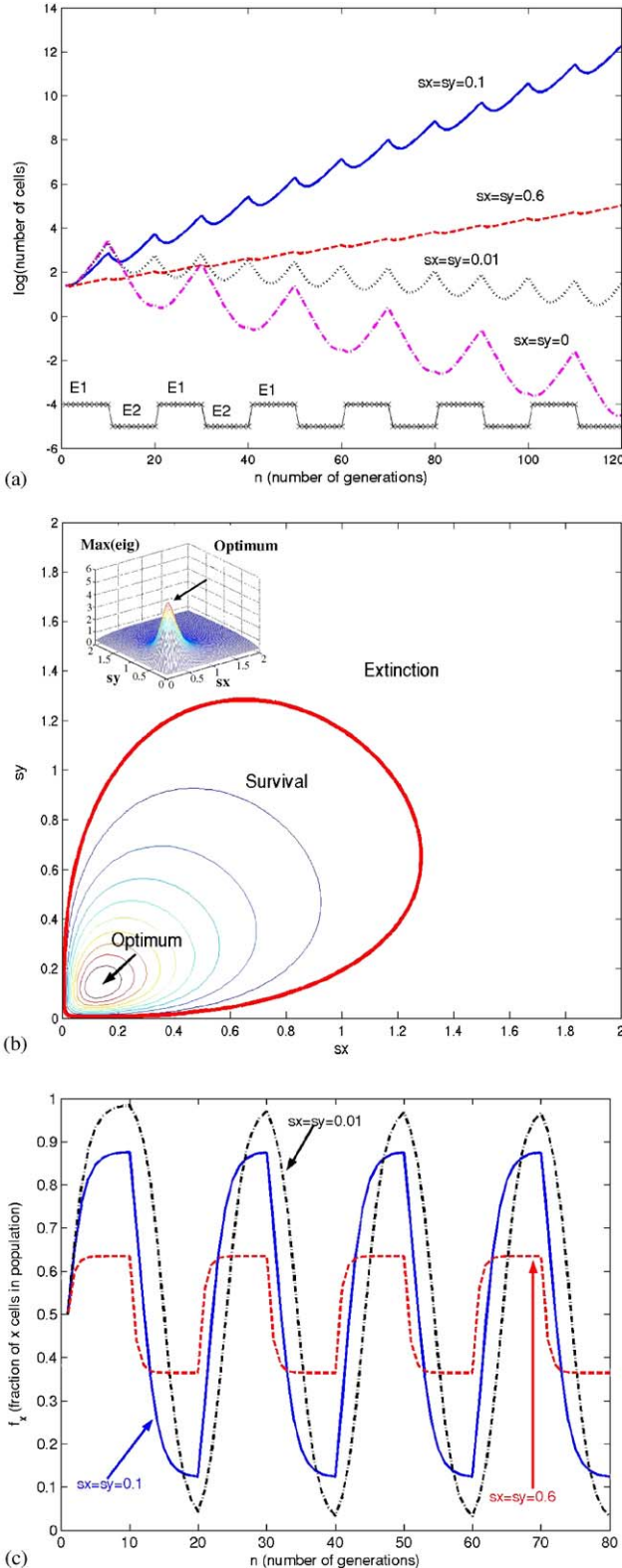


Fig. 3. *RPV* cell state switching rates can be too fast, too slow, or optimal: (a) With no cell state switching, the population quickly goes extinct ($sx = sy = 0$, purple curve). If cell state switching rates are too slow, the population still dies out, but more slowly ($sx = sy = 0.01$, grey curve). At the optimal cell state switching probability rates, the population proliferates at its maximal rate ($sx = sy = 0.1$, blue curve). If switching rates are too fast, the growth rate declines ($sx = sy = 0.6$, red curve). (b) Contour and mesh (inset) plots showing the long-term growth rate of the population (maximal eigenvalue of $R_{1d}^{N1} R_{2d}^{N2}$) as a function of switching rates sx and sy . Outside the red ‘survival’ curve, the population has a negative growth rate ($\text{Max}(eig) < 1$). Inside this curve, it has a positive growth rate ($\text{Max}(eig) > 1$). The maximal, *ESS* value occurs at $sx = sy \approx 0.1$. (c) Population composition f_x ($= x / (x + y)$ = number of x cells in the population / (total number of x and y cells)) as a function of time for different cell state switching rates (sx, sy). At slow switching rates, the steady-state population composition approaches the ideal of all- x in $E1$ ($f_x = 1$) and all- y in $E2$ ($f_x = 0$), but the time it takes to reach this steady state is detrimentally slow ($sx = sy = 0.01$, black curve). At fast switching rates, the steady state population composition is far from the ideal, but convergence time to this steady state is fast ($sx = sy = 0.6$, red curve). The optimal cell switching rates balance the benefits of fast convergence to steady state with the costs of non-optimal steady-state composition most advantageously ($sx = sy = 0.1$, blue curve). For these plots, the environment is periodic, alternating between 10 generations spent in $E1$ and 10 generations spent in $E2$ ($N1 = N2 = 10$). Growth rate parameters are as in Fig. 2

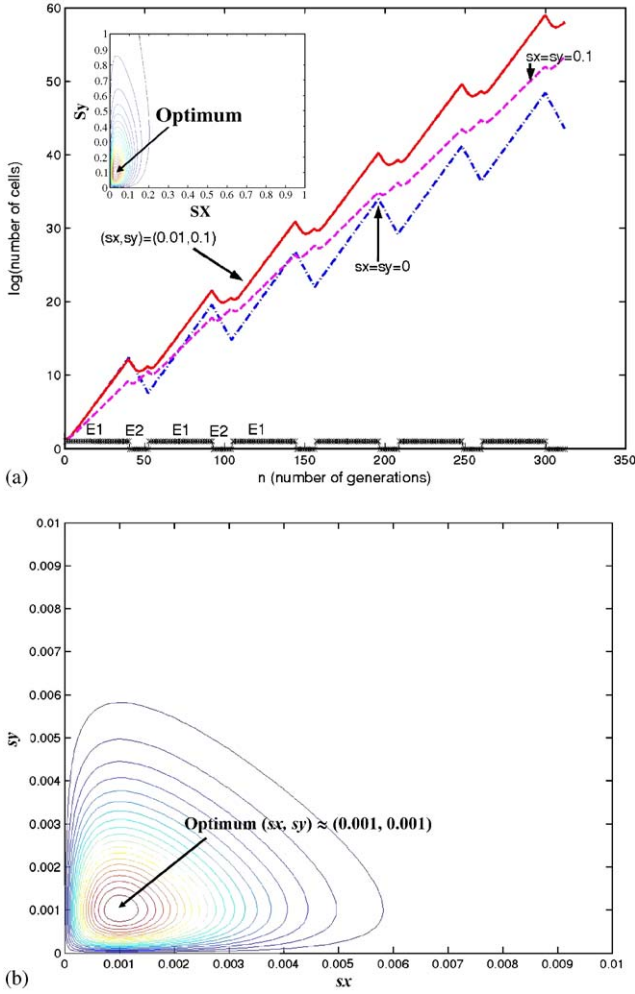


Fig. 4. Optimal switching rates depend on environmental lifecycle asymmetries and environmental autocorrelation: (a) Asymmetric lifecycles yield mirror asymmetric optimal switching rates. A lifecycle alternating between $N_1 = 40$ generations in E_1 and $N_2 = 12$ generations in E_2 has optimal switching rates of $(s_x, s_y) \Rightarrow (0.01, 0.1)$ (red curve). Note that $N_1/N_2 > 1 \Rightarrow s_y/s_x > 1$. (b) The higher the environmental autocorrelation or lifecycle period, the slower the optimal switching rates. A lifecycle alternating between 1000 generations in E_1 and 1000 generations in E_2 has optimal switching rates of $(s_x, s_y) \approx (0.001, 0.001)$, in contrast to the faster optimum shown in Fig. 3b with $N_1 = N_2 = 10$. Growth rate parameters are as in Figs. 2 and 3.

switching rates can slow growth or lead to extinction because though the convergence rate to steady state is accelerated by fast switching, generally of benefit to the long-term growth rate of the population, this accelerated convergence is achieved at the expense of a suboptimal steady state population composition. If switching rates are extremely fast, the steady-state composition $f_{x_i}(SS)$ approaches $s_y/(s_x + s_y)$, $(f_{x_i}(SS) = \lim_{t \rightarrow \infty} (\# \text{ cells expressing } x) / (\text{total } \# \text{ cells}) \text{ in environment } E_i)$, a composition far from the ideal of being all- x in E_1 ($f_{x_1}(SS) = 1$) and all- y in E_2 ($f_{x_2}(SS) = 0$). At a composition approaching $s_y/(s_x + s_y)$, the total growth

rate of the population in E_i approaches $g_i(RPV') = g_{x_i}f_{x_i}(SS) + g_{y_i}(1 - f_{x_i}(SS)) = g_{x_i}(s_y/(s_x + s_y)) + g_{y_i}(s_x/(s_x + s_y))$. Extinction results if $\prod_{j=1}^m g_j(RPV')^{n_j} < 1$. If, for example, $g_{x_1} = g_{y_2} = 1.3$ and $g_{y_1} = g_{x_2} = 0.6$, fast symmetric switching rates lead to extinction because $g_1(RPV') = g_2(RPV') = (g_{x_1} + g_{y_2})/2 = 0.95$.

At very slow switching rates, the steady-state composition in each environment can approach the ideal, e.g. $f_{x_1}(SS) \rightarrow 1$ and $f_{x_2}(SS) \rightarrow 0$. However, the time it takes to reach this optimal composition can be long. So long, in fact, that if the cell state transition rate is very slow relative to the environmental transition rate, the environment can repeatedly cycle between opposing environments without cell state switching occurring, and thus ‘miss’ environmental transitions and the growth boost afforded to the preferred cell states. Even if environmental transitions are not missed, as in Fig. 3c, a growth rate deficit accrues during the time spent converging to the steady-state composition, resulting in a loss of fitness.

Thus, optimal switching rates are those that most advantageously balance the benefits of fast convergence with the costs of non-optimal steady-state composition, a fulcrum largely determined by environmental autocorrelation and asymmetries. Large environmental autocorrelations imply lengthy stays in a single environment, meaning that the population will be at its steady-state composition $f_x(SS)$ most of the time in many environments. In such a lifecycle, the benefits of having a near-optimal $f_x(SS)$ dominate the cost of slower convergence to steady state, and the optimal switching rates are quite slow. Whereas if environmental autocorrelations are such that the time scale of environmental transitions is close to that of the growth rates of the selected cell state in each environment, the benefits of fast convergence to f_{x_i} outweigh the costs of sub-optimal f_{x_i} , and optimal switching rates are relatively fast. For example, $(s_x, s_y)_{opt} \approx (0.9, 0.9)$ if $N_1 = N_2 = 2$ (N_i = the number of generations spent in E_i), whereas if $N_1 = N_2 = 1000$ (assuming identical growth rates in E_1 and E_2), $(s_x, s_y)_{opt} \approx (0.001, 0.001)$ (Fig. 4b). For periodic environments, optimal switching rate magnitudes are on the order of $1/N$, where $N = N_1 + N_2$ is the environmental lifecycle period, an observation supported by analytical work by Lachmann and Jablonka (1996). However, optimal switching rates tend to be relatively slower in the Markov environment case, even if the mean amount of time spent in each environmental state is the same as for the periodic case. If the lifecycle is skewed to spend more time in E_1 (selecting for x and against y) than E_2 (selecting for y and against x), or if the growth rate of x in E_1 exceeds the growth rate of y in E_2 , then $(s_y/s_x)_{opt} > 1$ to ‘take advantage’ of the environmental asymmetry (Fig. 4a). The skewed switching rates provide a growth rate boost in the dominant environment E_1 at the expense of a

growth rate deficit in $E2$, with the overall effect being a maximization of the long-term growth rate of the population (but not a minimization of growth rate variance, as discussed below). These dependencies provide clues on the origins of switching rate profiles and the multiplicity of mechanisms seen in randomly phase varying populations (see Section 4).

Stockbrokers in the dish: RPV can minimize growth rate variance and extinction probability, even when it does not maximize growth rate. Theorem 1 concerns the extreme scenario of a lifecycle with such stringent and opposite selective criteria that no cell can hope to survive without the benefit of RPV (i.e. $(g_{i1})^{\pi_1}(g_{i2})^{\pi_2} \dots (g_{im})^{\pi_m} < 1$, for all cell states i). Is RPV still advantageous under less stringent selection? Numerical investigations suggest that if the selective forces over the lifecycle, while oppositely oriented, are less extreme, admitting a positive long-term growth rate to pure, non-phase varying populations (e.g. $(g_{i1})^{\pi_1}(g_{i2})^{\pi_2} \dots (g_{im})^{\pi_m} < 1$, for at least some cell states i), RPV still maximizes long-term growth rate if the lifecycle is symmetric or near-symmetric, or if the lifecycle is strongly asymmetric but the environmental autocorrelation or lifecycle period is high (Fig. 4).

If, however, the lifecycle is strongly asymmetric and the environmental autocorrelation or lifecycle period is relatively short, RPV may no longer maximize the expected long-term growth rate of the population (as measured by the maximal eigenvalue in deterministic environments or the Lyapunov exponent in stochastic environments). In this case, the expected long-term growth rate of a monomorphic, non-phase varying population exceeds that of random phase variable cells. If, for example, the population spends about 50 generations in $E2$ for every 5 generations spent in $E1$ ($p_{1,2} = 0.18$; $p_{2,1} = 0.02$), the Lyapunov-exponent maximizing strategy is for the population to be all- y , the selected state in $E2$ (Fig. 5a). However, in stochastic environments, there is more to fitness than long-term growth rate as measured by the Lyapunov exponent $\log(\lambda_s)$ (see Section 2). Arguably, contemporary bacterial species are contemporary because their phenotype expression strategy minimizes the risk of extinction rather than simply maximizing growth. If so, then one might imagine a fitness function that captures not only the long-term risk of extinction due to out-competition from mutants (maximizing $\log(\lambda_s)$) or the risk of extinction due to the cell vs. (random) nature aspect of the game (minimizing $\exp(\log(\lambda_s)\log(\theta)/\sigma^2)$ if $\log(\lambda_s) > 0$,

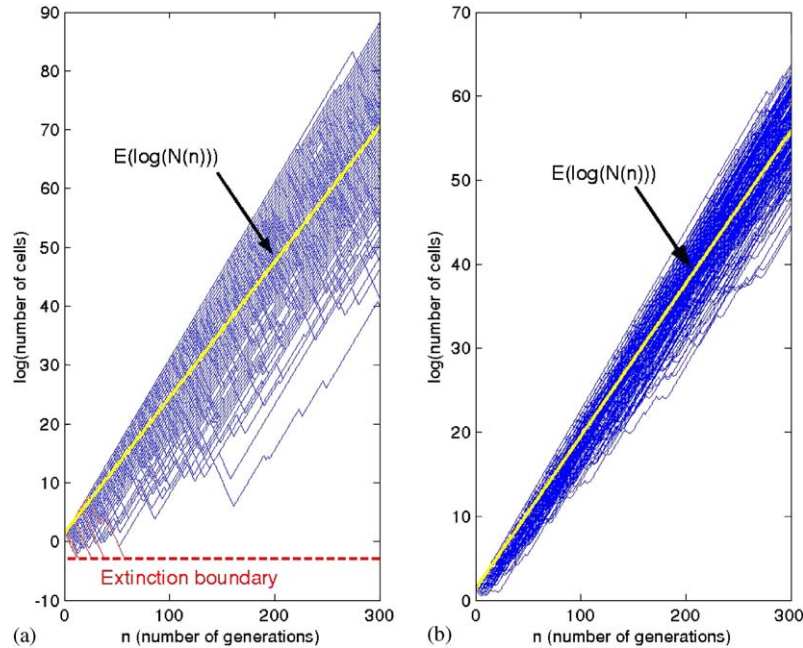


Fig. 5. RPV can minimize the growth rate variance and the probability of extinction due to ‘unlucky’ environmental trajectories, even when it does not maximize the stochastic growth rate (and thus is not considered ESS). Though a pure strategy, all- y population in an asymmetric Markov Environment cycling between $E1$ and $E2$ with transition probability rates $p_{1,2} = 0.18$ and $p_{2,1} = 0.02$ has a higher Lyapunov exponent ($\log(\lambda_s)_{pure} = 0.2305 \pm 0.0024$, yellow line in (a)) than does a randomly phase varying population with switching rates $s_x = s_y = 0.1$ ($\log(\lambda_s)_{RPV} = 0.1814 \pm .0011$, yellow line in (b)), it also has a much higher growth rate variance σ^2 than the RPV population ($\sigma_{pure}^2 = 0.1048$; $\sigma_{RPV}^2 = 0.0338$). This larger growth rate variance and the high death rate in $E1$ makes the pure strategy more vulnerable to rare environmental trajectories, as evidenced by the 4/200 trajectories leading to extinction shown in (a), in contrast to 0/200 extinction events for the RPV population shown in (b). Growth rates are as in Fig. 2; for each trajectory, the starting probability of being in each environmental state is set to the stationary distribution $pE1(0) = 0.1$ and $pE2(0) = 0.9$; the starting population size is 4, and the extinction threshold is set at 0.05.

where σ^2 is the growth rate variance and θ is the ‘quasi-extinction’ population density (Lande and Orzack, 1988; Caswell, 2001, p. 445)), but one that reflects all the risks inherent to the game of survival pitting cell against cell, and cell against nature, probabilistically weighted over all relevant time scales. Without knowing the exact form of this fitness function, one can conjecture that it will strike a balance between maximizing long-term growth rate $\log(\lambda_s)$ and minimizing the growth rate variance σ^2 and perhaps higher-order moments (see Doebeli, 1995), as do stock market investment strategies.

Whether operating with no information or noisy estimates, there is a parallel between cellular diversification strategies and stock portfolio investment strategies, where cells are dollars, cell states are stocks, and return is the long-term growth rate of the population. Stock market investors choose investment strategies based on a desire to maximize expected profit subject to some tolerance for risk. It is a well-known principle, and common practice, that diversification of a portfolio produces the minimum risk for a given expected long-term return on an investment (Merton, 1982). *RPV* (and sensor-triggered diversification, described in the next section) can be understood as different types of portfolio rebalancing, the frequency and probability distribution of which depend upon how good one’s information is about the environment, or ‘market’, and on ‘market’ dynamics. As in the stock market, numerical investigation reveals that even in lifecycles for which *RPV* does not maximize long-term (stochastic) growth rate, for instance those with strongly asymmetric lifecycles as presented above, *RPV* can minimize growth rate variance and ensure the existence of subpopulations with positive growth rates in all environments, thereby potentially minimizing the risk of being extinguished by rare catastrophic environmental trajectories. For example, though a pure strategy, all- y population has a higher Lyapunov exponent in a Markov environment cycling between $E1$ and $E2$ with transition probability rates $p_{1,2} = 0.18$ and $p_{2,1} = 0.02$ than does a randomly phase varying population with $sx = sy = 0.1$ ($\log(\lambda_s)_{pure} = 0.2305 > \log(\lambda_s)_{RPV} = 0.1814$), it also has a much higher growth rate variance σ^2 than does the *RPV* population ($\sigma_{pure}^2 = 0.1048 > \sigma_{RPV}^2 = 0.0338$).

A strategy that minimizes growth rate variance is a type of *security strategy* rendering the population relatively *indifferent* to the environmental trajectories produced by an opposing player, nature. Intuitively, *RPV* can minimize the growth rate variance because the growth rate of an *RPV* population is slower than that of the quickly growing pure- y population while in $E2$, but faster than that of the quickly dying pure- y population while in $E1$, thereby ‘closing the growth rate gap’ between the two environmental states. The larger growth rate variance of pure strategists, and—more to the point—the fast kill-rate of y cells in $E1$, makes the

pure strategist population more vulnerable to rare environmental trajectories when the starting population size is small than is an *RPV* population. This point is illustrated in Fig. 5 by the 4/200 trajectories leading to extinction of a pure-strategist population, in contrast to 0/200 extinction trajectories for the *RPV* population. Simulations like these suggesting a greater likelihood of extinction are supported by an application of Lande and Orzack’s approximation of the extinction probability of a population growing in a stochastic environment as a direct function of the ratio $\sigma^2/\log(\lambda_s)$; the inequality $\sigma_{pure}^2/\log(\lambda_s)_{pure} = 0.4547 > \sigma_{RPV}^2/\log(\lambda_s)_{RPV} = 0.1863$ indicates that a pure, all- y population is more likely to go extinct due to environmental stochasticity than is the *RPV* population, even though by virtue of its larger Lyapunov exponent it should be able to invade any *RPV* population and would be considered *ESS* by most analysts.

Interestingly, even when the environmental and sensing profile is such that *RPV* maximizes growth rate *and* minimizes variance (thereby both allowing *RPV* to invade any pure population *and* minimizing the probability of extinction due to environmental variation), the exact, ‘optimal’ switching rates for each objective differ; switching rate asymmetries mirror lifecycle asymmetries if growth rate $\log(\lambda_s)$ is being maximized (e.g. $\pi_1 = \pi_2$ & $g_{x1}/g_{y2} > 1 \Rightarrow (sy/sx)_{\sigma_{opt}} > 1$), whereas they are faster and inversely related to lifecycle asymmetries if variance σ^2 is being minimized (e.g. $\pi_1 = \pi_2$ & $g_{x1}/g_{y2} > 1 \Rightarrow (sx/sy)_{\sigma_{opt}} > 1$) (data not shown). Because *RPV* can minimize growth rate variance even when it does not maximize long-term growth rate, the net effect of incorporating growth rate variance into a definition of fitness and thus *ESS*—aside from shifting the optimal switching rates—is to expand the range of lifecycles and sensor profiles giving rise to *RPV*.

We conclude that in highly asymmetric lifecycles that are not highly autocorrelated, a pure strategy (maximizing stochastic growth rate) is likely able to invade an *RPV* population. However, pure strategists can also be more vulnerable to extinction due to ‘unlucky’ runs in the environment. In contrast, an *RPV* population is vulnerable to invasion by pure strategists, but is relatively protected against unexpected environmental trajectories. How evolution might balance this trade-off between vulnerability to mutant invasion and vulnerability to environmental uncertainty is unclear.

Time varying selection over the population is required for RPV selection: Thus far, we have focused on time varying environments, wherein different environmental states select for different cell states. Infection processes, however, usually involve cells moving from the outside to the inside of a host, and once inside, from host compartment to host compartment. To investigate whether a spatial, asynchronous version of the Devil’s Compromise scenario selects for random phase varying

phenotypes, as does the temporal, synchronous version explored elsewhere in this paper, we constructed a number of models (see Appendix B for a low-dimensional one). As in the synchronous Devil's Compromise scenario, this class of lifecycle (and model) comprises a number of different environmental states, each selecting for and against different (opposite) cell states. However, individual cells move asynchronously from (spatially discrete), *time-invariant* environment to environment according to a Markov process, rather than having the entire population simultaneously subject to a time-varying environment that transitions between environmental states in a Markov fashion (see inset in Fig. 6 for illustration). To our surprise, we found that *RPV* does not maximize growth rate in this type of lifecycle. A maximal eigenvalue mesh plot for the equations in Appendix B, which describe a simple, two-environment, two-cell state version of asynchronous, spatial Devil's Compromise scenario, illustrates that the *ESS* strategy is a non-phase varying polymorphism ($s_y = 0$ and/or $s_x = 0$) rather than *RPV* ($s_x > 0$ and $s_y > 0$) (Fig. 6).

Mathematically, one can reason about the differences between synchronous temporal and asynchronous spatial Devil's Compromise lifecycles by comparing their growth exponents (dominant eigenvalues). Growth exponents are derived from a matrix product in the former, and from a single, higher-dimensional matrix in the latter (see Section 5). *RPV* can render the eigenvalues of the matrix products larger than the product of the eigenvalues from each matrix, whereas

the eigenvalues of the single, large matrix for the asynchronous case can never be larger than in the pure strategy case.

A more intuitive explanation derives from a consideration of the costs and benefits of *RPV*. The only conceptual difference between the temporal and spatial versions of the Devil's Compromise, as we have defined them, is that in the former, the variable selective forces are applied synchronously to the entire population, whereas in the latter, variable selective forces are applied asynchronously to individual cells. In the spatial, asynchronous version of the Devil's Compromise, *RPV* exacts a cost: the conversion of cells in a favored cell state to unfavourable cell states reduces the growth rate of the population in each environment of the lifecycle. However, unlike the synchronous Devil's Compromise scenario, these costs are not outweighed by benefits. Because each spatially distinct environment is time-invariant, promoting growth of the same favored cell state without interruption, there is no need to create an 'artificial' reservoir of favored cell state subpopulations to populate each environment. If seeded by an initial population heterogeneity (polymorphism), favoured cell state subpopulations are maintained in each environment. This example illustrates the principle that it is selection over the *population*, as generated by a *time-varying environment* acting on cells without environmental sensors that selects for phase varying phenotype expression. Time-invariant, density independent environments, and asynchronous variable selection over individual cells do not suffice. From these examples, we conclude that that though the lifecycles of randomly phase varying pathogens have a spatial component, they must also be subject to time-varying selective forces acting synchronously or near-synchronously on the population. Such population level selection could be a product of time-varying selection within different spatial locations, or, alternatively, from near-synchronous movement of subpopulations from locale to locale (see Section 4). For a treatment of diploid polymorphism in temporally and spatially varying environments, see Gillespie (1975).

3.2. Phase variation with imperfect sensors in a time-varying environment

Most realistic models of signal transduction fall somewhere in between the extremes of perfect and absent environmental sensors. There is evidence that at least some *RPV* is tuned to environmental conditions. For example, the switching rates and type 1 piliation level of uropathic *E. coli* populations are temperature and medium dependent. On-to-off switching of pili expression can be fast (0.3/cell/gen in rich medium by some estimates) or slow (0.001/cell/gen in poor nutrient medium), with off-to-on switching rates peaking at

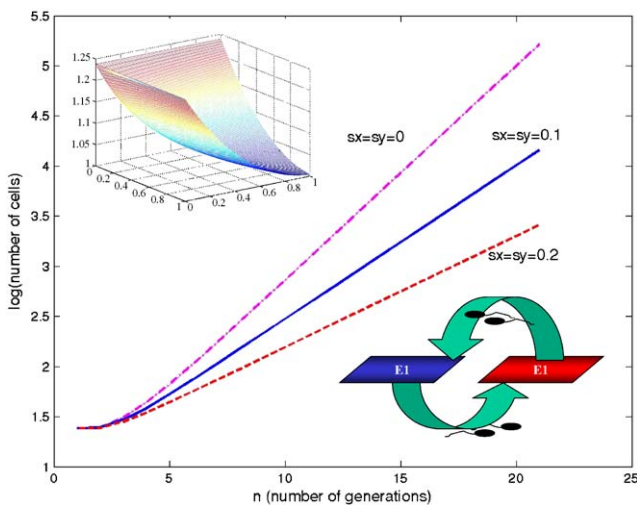


Fig. 6. *RPV* (red and blue trajectories) does not maximize growth rate in a spatial, asynchronous version of the Devil's Compromise scenario. A polymorphism (pink curve, at $s_x = s_y = 0$) is *ESS* when individual bacterial cells move asynchronously from environment to environment according to a Markov process. For this plot, growth rates $\lambda_x(2) - \mu_x(2) = \lambda_y(1) - \mu_y(1) = -0.4$ and $\lambda_x(1) - \mu_x(1) = \lambda_y(2) - \mu_y(2) = 0.3$; $\Delta t = 1$; and $m_{1,2} = m_{2,1} = 0.1$ in Eq. (5). Insets are the maximal eigenvalue mesh plot (upper), and an illustration of cells moving asynchronously between spatially discrete environments (lower).

mammalian host body temperature (Gally et al., 1993) (see (Saunders et al., 2003) for an updated technique for measuring *RPV* switching rates and possible caveats for currently measured switching rates). Presumably, this environmental modulation creates piliated populations in the bladder and unpiliated populations outside the host, where they are less useful. Similarly, *Staphylococcus aureus* uses cell density and environmental signals to control the expression of toxins, adhesins, and capsular proteins, allowing for coordinated virulence factor expression within a host.

In this section, we look at different types of sensor defects (unobservable environmental transitions, incorrect identification of environmental states, signal transduction delays, and additive noise), and different classes of environments, and analyse for combinations that give rise to *RPV* as an ESS. Because *RPV* is selected for if cells have no sensors and live out a time varying, Devil's compromise lifecycle (see previous section), we expected that significant sensing defects of any type would select for *RPV* in equivalent environmental conditions. We envisioned a transition from a 'sensor-based pure' strategy (If environmental sensors read $\vec{E} = E1$, express cell state x : ELSE, express y) to an *RPV* strategy as sensor goodness declined. To our surprise, we found that not all types of sensor defects give rise to *RPV* in Devil's Compromise time-varying scenarios, even if those defects are extreme. Only sensor defects rendering a subset of environmental transitions *unobservable* to the cell with high probability, or long signal transduction delays relative to the timescale of environmental change (in effect simulating unobservability), select for *RPV*. In the two-environment, two cell state example modelled by Eq. (1) (with other parameters listed in the caption of Fig. 7), for instance, random phase varying expression of x and y phenotypes maximizes growth rate only if environmental transitions between $E2$ and $E1$ are observable with probability less than 0.2 (see Fig. 7 and 10a,b). With just slightly more observable environmental transitions, no amount of additive noise or inaccuracy in identifying new environments resulted in a survival advantage for *RPV* strategists.

Though we did not prove it for the general case of arbitrarily many cell states and environmental states (as we did in Theorem 1), a large number of numerical experiments, conducted as described in Section 5, support the conjecture that *RPV* is ESS if the likelihood of cycling through a set of states satisfying the Devil's compromise is high, and if the probability of the sensor being able to observe environmental transitions within this set is low. Intuitively, if there are unobservable transitions between environmental states with opposing selective criteria, *RPV* reduces the risk of extinction by protecting against the event that the environment cycles between these unobservable states for an extended period of time.

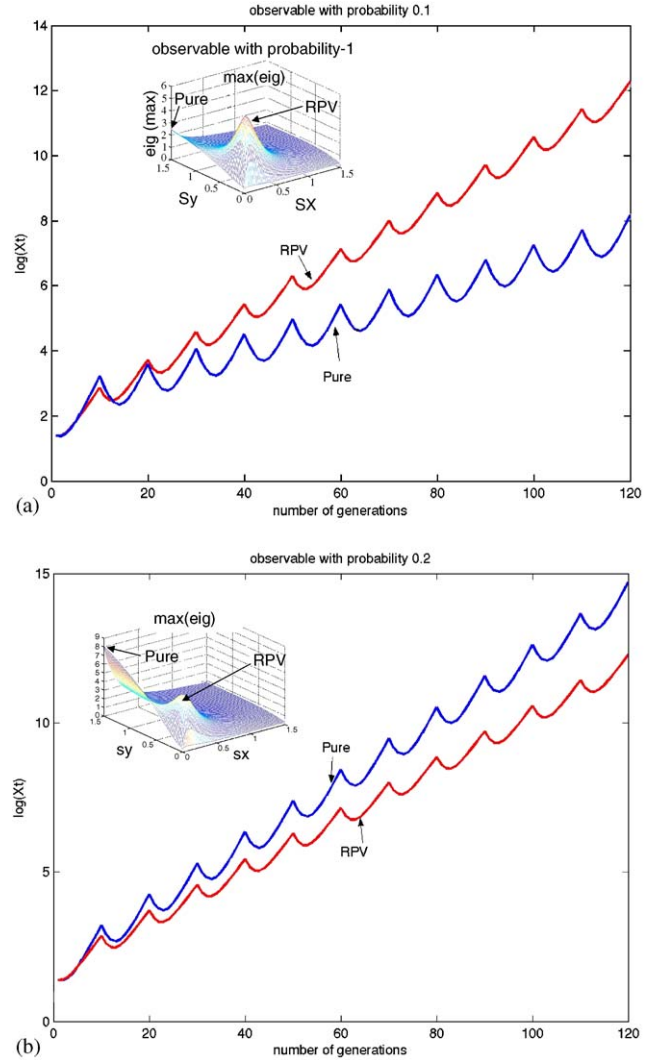


Fig. 7. *RPV* with imperfect environmental sensors. If cells have environmental sensors with a defect that renders a subset of environmental transitions unobservable with high probability, *RPV* between 'selected' cell states in this set can maximize expected long-term growth rate: (a) *RPV* (red) out-competes a sensor-based pure strategy (blue), if environmental transitions are observable with probability 0.1. Inset is a mesh plot of long-term growth rate (Malthusian exponent) as a function of switching rates ($sx1, sy1$). The maximum occurs at an *RPV* strategy with $sx1 = sy1 \approx 0.1$. (b) At higher levels of observability ($pObs \geq 0.2$), a sensor based pure strategy (blue) outcompetes a *RPV* strategy (red). Note that $sx = 0$ at the optimal growth rate (we set $sx = sx1 = sy2$ and $sy = sy1 = sx2$ in the inset mesh plot). Parameters $ps11 = ps22 = 1$ (accuracy is maximal), $rate = 0$ (there is no additive noise), $N1 = N2 = 10$; and all other parameters are as defined in Fig. 3.

A sensor-based mixed strategy: Other types of sensor defects introduce other adaptations. One such adaptation results from sensors that can reliably detect environmental transitions, but have poor precision in identifying new environments (and thus do not 'know' the best cell state for a new environment). This type of sensor defect can give rise to a strategy that

probabilistically diversifies the population into different cell state subpopulations upon entry into a new environment, a *sensor-based, mixed* strategy that looks very much like heterogeneous stress response deployment in *B. subtilis* (Msadek, 1999), or the partitioning of stressed bacterial populations into lysing ‘donor’ and DNA or nutrient uptake ‘recipient’ subpopulations (Steinmoen et al., 2002; Gonzalez-Pastor et al., 2003; Webb et al., 2003). More precisely stated, a sensor-based mixed strategy takes a noisy measurement of environmental state and maps it onto a cell state probability (e.g. if the sensor reads (*environmental transition, new environment* = E_i) then express x with probability P_i and y with probability $1 - P_i$). Environmental transitions could be sensed through signal-integrating switches or pulse generator circuitry, as in the SigB controlled general stress response in Gram positive bacteria (Hecker and Volker, 2001). Below, we formally prove that if cells with an arbitrary number of cell states have sensors that can sense environmental transitions, a sensor-based mixed strategy can out-compete an *RPV* strategy, even one that ‘recalibrates’ switching probabilities upon entry into a new environment.

Theorem 2. (A sensor-based mixed strategy can out-compete *RPV* or pure strategies if cells have sensors that can detect environmental transitions).

Consider a third population of bacteria in addition to those defined in Theorem 1, P_3 , that has partial sensors: they can sense environmental transitions but not the environment itself. Assume that population P_3 uses this information as follows: at each environmental transition, for $1 \leq i \leq k$, the subpopulation in cell state s_i divides into the k cell states in the following proportions: α fraction switches to cell state s_j , for $j \neq i$, and the remaining $(1 - (k-1)\alpha)$ fraction remain in cell state s_i ; α is as defined in Theorem 1. We will say that P_3 follows a sensor-based mixed strategy.

In the setup of Theorem 1 let us make the additional assumption that in each environment there is a unique cell state with the highest growth rate. Then the growth rate of P_3 , the sensor-based mixed strategy population, dominates that of P_2 , the randomly phase varying population.

Proof. See Appendix A.

The assumption in Theorem 2 that there is a unique strategy having the highest growth rate can be dispensed with by considering, in each environment, all strategies having the highest growth rate. The argument in the proof essentially points out that in the presence of partial sensors that can sense environmental transitions, *RPV* only depletes the preferred subpopulation in each environmental state and hence a sensor-based mixed strategy dominates

a sensor-based *RPV* strategy.

Observe that in Theorem 2, the sensor-based mixed strategist population P_3 can utilize information on environmental transitions even more effectively if instead of dividing in proportions specified above, it divides in proportions determined by growth rates and times spent in various environments, and makes use of noisy estimates of environmental state should they be available. Evolution by natural selection would arrive at these optimal rates. For example, with sensors rendering environmental transitions observable ($p_{Obs} = 1$), but environmental identification accuracy low ($(ps11, ps22) = (0.6, 0.6)$), the *ESS* for our two cell state, two environment population (Eq. (1)) living an asymmetric lifecycle that alternates between spending 50 generations in $E1$ and 3 generations in $E2$ is as follows: express x with probability $p1 \approx 0.4$ and y with probability $(1 - p1) \approx 0.6$ upon an environmental transition, if the environmental state estimate reads $\vec{E} = E2$; express x with probability $p1 = 1$ upon an environmental transition should the estimate be $\vec{E} = E1$ (see Fig. 8a). Note that optimal mixture probabilities reflect lifecycle asymmetries in a sort of ‘rich get richer’ fashion, biasing the population composition in favor of those cell states selected by dominant environmental states.

A low-pass filtered pure strategy. Other sensor defects, such as additive noise or mildly defective observability and accuracy, mostly select for a sensor-based pure strategy. For cells with sensors that are reasonably good at identifying environmental transitions and environmental states, a sensor-based pure strategy (If $\vec{E} = E1$, express x : *ELSE*, express y) can out-compete random phase variable or sensor-based mixed strategies (Figs. 7b, 8b and 10), even though all populations would appear somewhat heterogeneous and phase variable under a microscope due to sensor noise. Because a pure strategy in the presence of noise is essentially a deterministic rule based on a noisy measurement, high-frequency noise on environmental sensors introduces the specter of detrimental high-speed cell state switching ‘chatter’. To counter this tendency, the *ESS* strategy in such noisy environments is pure but with a twist in the form of *low-pass filtering*. Bacterial signal transduction can be very fast, on the order of milliseconds (from ligand binding to response regulator modification in a two component system (Grimshaw et al., 1998; Stewart and Van Bruggen, 2004)), or on the order of 30 min or more if the ‘output signal’ is defined as multiple transcriptional events downstream of a signal transduction pathway (McClure, 1980; McAdams and Arkin, 1997). A low-pass filtered pure strategy, a signal transduction network design with built-in inertia in processing and responding to environmental signals, has a noise-filtering effect that increases the long-term growth rate of the population in noisy environments

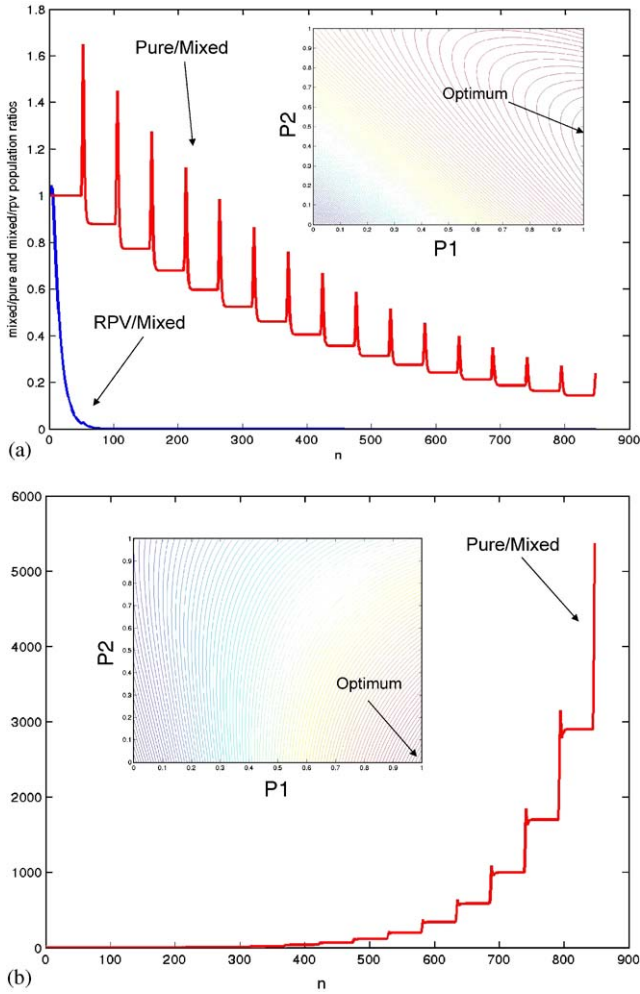


Fig. 8. Sensor defects giving rise to sensor-based mixed and pure strategies: (a) If cells growing in asymmetric Devil’s Compromise lifecycles have environmental sensors that can reliably detect environmental transitions, but have poor accuracy in identifying new environments, a sensor-based mixed strategy out-competes a sensor-based pure strategy (red) or an *RPV* strategy (blue) (sensor accuracy is $(ps_{11}, ps_{22}) = (0.6, 0.6)$). Notice the optimal mixing probabilities $(P_1, P_2) = (1, 0.4)$. (b) With reasonably accurate sensing, pure strategy cells win out (the optimal mixing probabilities are $(P_1, P_2) = (1, 0)$, a sensor-based pure strategy). Inset figures are contour plots of long-term growth rate as a function of mixing probabilities. All parameters are as in Fig. 3 except for the asymmetric lifecycle defined by $N_1 = 50$ and $N_2 = 3$ (the population alternates between spending 50 generations in E_1 and 3 generations in E_2).

over that of a fast-responding pure strategy or any other competing strategy. For example, with sensors rendering environmental transitions reasonably observable ($pObs = 0.6$), and environmental identification reasonably accurate ($(ps_{11}, ps_{22}) = (0.8, 0.8)$), but with significant additive noise ($rate = 1$), the *ESS* for our two cell state, two environment population (Eq. (1)) is a low pass filtered pure strategy with transition rates ($sx_1 = sy_2 = 0.3, sy_1 = sx_2 = 0$) (Fig. 9). The low-pass filtering is evident from the local maximum in growth rate at the

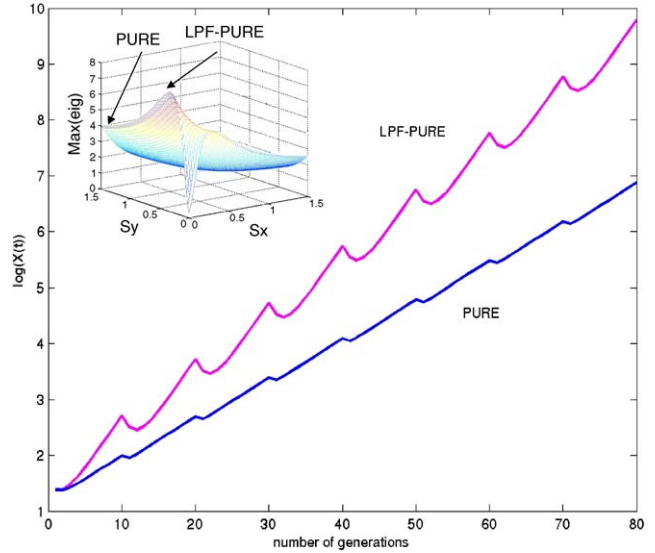


Fig. 9. Low-pass filtering increases fitness if additive noise level is high. A low-pass filtered sensor-based pure strategy (magenta; $sx_1 = sy_2 = 0.3, sy_1 = sx_2 = 0$) outcompetes a pure strategy with a faster response time (blue; $sx_1 = sy_2 = 1.5, sy_1 = sx_2 = 0$). Inset is a mesh plot of long-term growth rate as a function of switching rates (sx_1, sy_1) , showing a maximum at the low-pass filtered pure strategy ($sx_1 = sy_2 = 0.3, sy_1 = sx_2 = 0$). Environmental and growth rate parameters are as in Fig. 3, with sensor parameters $pObs = 0.6, ps_{11} = ps_{22} = 0.8$ and additive noise rate = 1.

relatively sluggish switching rate of ($sx_1 = sy_2 = 0.3$) (Fig. 9, inset); without additive noise, the faster the cell state switching rate is upon entry into a new environment, the better (Fig. 7b). Just as there is a Nyquist rate guide to sampling rates in electronic signal processing (Oppenheim et al., 1983), there is a ‘best’ signal transduction speed and post-processing profile in bacteria that is fast enough to optimize cell proliferation in a noisy time-varying environment, but not so fast as to trigger excessive, detrimental phenotype switching in response to noise. The growth advantage conferred by low-pass filtering is even more pronounced if cell state switching costs are explicitly taken into account (see modeling section and Appendix D).

An ESS bifurcation plot: Evolutionarily stable strategies depend on a population’s sensor-defect profile and on the environment in which the population lives. A population living a Devil’s Compromise time-varying lifecycle with sensors unable to sense environmental transitions over an ‘extinction set’ can be expected to exhibit *RPV* over the extinction set, though perhaps not outside of this set. A population with sensors able to sense environmental transitions but unable to correctly identify new environments will exhibit a probabilistic, sensor-based mixed strategy, diversifying upon entry into a new environmental state (if the lifecycle is asymmetric). If those sensors provide a decent ‘guess’ at environmental location, in addition to signaling

environmental transitions, the *ESS* is a pure, deterministic strategy based on a potentially noisy signal. If the signal is too noisy, the *ESS* adaptation is a low-pass filtered pure strategy—signal processed deterministic regulation driven by a noisy input—or a low-pass filtered mixed strategy, should sensor accuracy be low. These observations distill into a map from the continuous space of sensor-defect profile to the discrete space of *ESS* class, predicated on particular environmental lifecycle conditions. A bifurcation plot, slices of which are shown in Fig. 10, is a visual aid to understanding this map, though the high dimensionality of the sensor-space undermines its utility to some extent (see Materials and methods for a description of *ESS* bifurcation plot construction). Note that the location of the boundaries between different *ESS*s depend upon lifecycle asymmetries and environmental autocorrelation. Strong lifecycle asymmetries bias the *ESS* toward a mixed strategy, requiring greater sensor accuracy to shift the *ESS* from mixed to pure. Conversely, less asymmetric lifecycles bias the *ESS* toward a pure strategy, even if the sensor accuracy is low.

Getting the most bang for your sensor buck: Considering that perfect sensing is likely expensive, if not impossible, the question arises as to what the best return might be on the sensor ‘dollar’. Is it better to have observable environmental transitions but poor accuracy in identifying environmental states, or unobservable transitions over a subset of environmental states but more precise estimates of environmental location? What is the cost in terms of fitness of different sensor deficits, and thus the direction of selective pressure in evolving new sensing capabilities? We investigated these questions (very simply) by constraining total sensor goodness to the sum $observability + accuracy = 1$ and determining what balance between environmental transition observability and environmental identification accuracy maximizes fitness as measured by the long-term growth rate of the population (Fig. 11; normalized parameters $observability = pObs$ and $accuracy = 2 \times (Ps_{ii} - 0.5)$). We found that in the absence of additive sensor noise, the sensor design that maximizes fitness spends every possible sensing ‘dollar’ on observability, and none on accuracy (Fig. 11, green curve). In the presence of sensor noise, dividing resources between observability and accuracy maximize fitness, with a greater share going to observability (Fig. 11, blue and red curves).

4. Discussion/conclusion

Microbial populations with different sensor profiles in the exact same environment will adopt different evolutionarily stable strategies, depending on the types of sensing failures they experience. We find that if cells

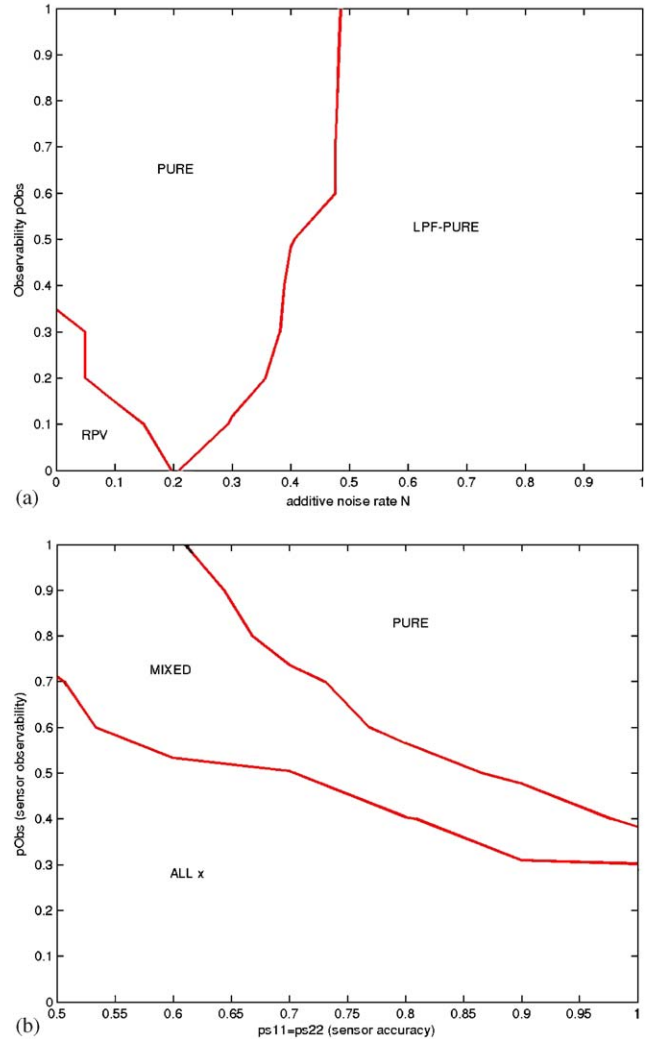


Fig. 10. *ESS* bifurcation diagrams. Evolutionarily stable strategies are a function of the selective forces over the lifecycle of the organism, and the ability of a cell to sense its environment. Thus, every point in the parameter space (E, Q) maps onto an *ESS*, where E is the parameter vector for the Markov process M or cycle times $(N1, N2)$ defining the environment, and $Q = (pObs_{ij}, Ps_{ij}, sq_{ij}(k))$; $i, j, k = 1 : 2$; is the parameter vector defining the environmental sensor. Though such a complete bifurcation diagram is too high-dimensional to show here, we show a few slices: (a) Bifurcation diagram showing the dependence of *ESS* on observability and additive noise. Sensor accuracy is $Ps_{ii} = 0.6$; $i = 1, 2$; and the lifecycle is symmetric ($N1 = N2 = 10$). (b) Bifurcation diagram showing the dependence of *ESS* on sensor accuracy Ps_{ii} and environmental-transition observability $pObs$, with no additive noise ($rate = 0$) and an asymmetric lifecycle defined by $(N1 = 50, N2 = 3)$. Notice transitions from sensor-based mixed, to pure, to *RPV*, to low-pass filtered versions of each strategy as the parameters vary.

are unlikely to sense environmental transitions or are subject to long signal transduction delays relative to the time-scale of environmental change, a *time-varying* environment can select for phase varying phenotype expression, *if* different environmental states select for different cell states. We call this scenario a *Devil's Compromise*, because *RPV* is neither optimal nor *ESS* in any one environmental state, yet it is required for

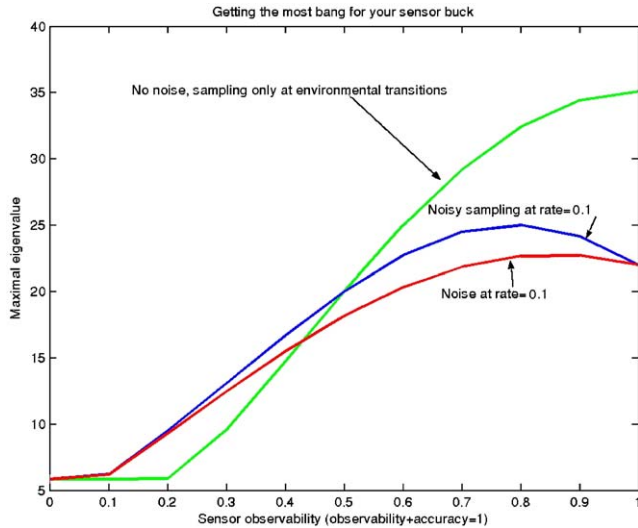


Fig. 11. Getting the most bang for your sensor buck. This plot shows maximal long-term growth rate of the population as a function of sensor accuracy and observability, with total sensor ‘goodness’ constrained by the equation $accuracy + observability = 1$. Thus, at one end of the sensing spectrum the cell registers environmental transitions but has no information about the identity of the environment ($observability = 1$, $accuracy = 0$), whereas on the other end of the spectrum $observability = 0$ and $accuracy = 1$. In the absence of additive sensor noise, every sensor ‘dollar’ should be spent on sensing environmental transitions and none on accuracy in identifying new environments (green curve: the optimum occurs at $(p_{Obs}, p_{s_{ii}}) = (1, 0)$). In the presence of additive noise, the optimal sensor design distributes sensor dollars between *observability* and accuracy, with greater weight placed on *observability* (red and blue curves: optima occur at $(p_{Obs}, p_{s_{ii}}) = (0.9, 0.6)$ and $(p_{Obs}, p_{s_{ii}}) = (0.8, 0.7)$, respectively). In these plots, $observability = p_{Obs}$, the probability of sensing environmental transitions ($p_{Obs} \in [0, 1]$), and $accuracy = 2 \times (p_{s_{ii}} - 0.5)$, where $p_{s_{ii}}$ = the probability that the sensor will read $q = Ei$ when the cell is in environment Ei ($p_{s_{ii}} \in [0.5, 1]$).

survival over the lifecycle of the organism. Alternatively, *RPV* can be viewed as effecting a Parrondo paradox (Harmer et al., 2001) wherein random alternations between losing strategies produce a winning strategy.

Optimal *RPV* cell state switching rates are fast enough to ensure the availability of high-fitness phenotypes to future environmental states, but not so fast as to unnecessarily drain the population of cells expressing high-fitness phenotypes in the current environmental state. Optimal switching rate magnitudes are inversely proportional to environmental autocorrelation, whereas optimal switching rate asymmetries mirror lifecycle asymmetries. Thus, an observation of *RPV* transition rates allows prediction of the temporal and probabilistic features of the lifecycle that gave rise to the strategy. Conversely, this linkage can serve as a guideline for designing time-varying environments to experimentally direct the evolution of particular *RPV* strategies, or to design an environment that ‘beats’ the bacterium at its game in health or bioremediation applications.

If cells have other sensor defects such as additive noise or environmental misidentification, *RPV* is not selected

in ‘Devil’s Compromise’ time varying environments. If, however, a population’s sensors can detect environmental transitions, but have poor precision in identifying new environments (and thus the optimal cell state), the *ESS* is to probabilistically diversify the population, a *sensor-based, mixed* strategy that looks very much like heterogeneous stress response deployment in *B. subtilis*. Bet hedging is a good metaphor for sensor-based mixed strategies; environmental transitions are signaled (initiation of a bet and race), but uncertainty about the new environment (winning horse) calls for diversification over phenotypes (competing horses) according to the probabilistic rule governing the lifecycle (odds).

In the presence of excess additive noise on an environmental signal, a sensor-based mixed strategy requires *low-pass filtering* to maintain evolutionary stability. Low-pass filtering of noisy signals is implemented in cells by cascades, negative feedback, feed-forward architectures (Mangan and Alon, 2003), hysteresis (Ferrell, 2002), orientational control of invertible DNA elements (Wolf and Arkin, 2002), and a variety of 1st, 2nd and 3rd order chemical reactions (Samoilov et al., 2002; Rao et al., 2002; Wolf and Arkin, 2003). With sensors that can identify environmental transitions and new environmental states with reasonable accuracy, the *ESS* is a sensor-based pure (deterministic) strategy, also low-pass filtered in the presence of additive noise. Even in lifecycles for which *RPV* does not maximize long-term growth rate, *RPV* can minimize growth rate variance and minimize the risk of being extinguished by rare, potentially catastrophic environmental trajectories. *RPV* minimizes growth rate variance by ‘closing the growth rate gap’ between different environmental states and protects against environmental fluctuations by seeding new environments with high-fitness phenotypes.

With the exception of the sensor-based pure strategy, the above diversification strategies have in common that they are not optimal or even *ESS* in any particular environmental state examined in isolation, though they maximize the long-term growth rate of the population as it moves through its lifecycle. In contrast, in Part II of this study (Wolf et al., 2005) we show that a frequency-dependent environment where the fitnesses of cell states are greatest when rare does select for diversification, even when viewed in isolation. Such environments support pure and *RPV* strategies polymorphically at the *ESS* composition and a non-*ESS* optimal *RPV* strategy playing the cooperator role in a modified game of Prisoner’s Dilemma. The population would be most fit in such an environment if all cells randomly phase varied at the optimal rate, but individual cells have a growth-rate incentive to defect (mutate) to other switching rates or non-phase variable phenotype expression, leading to an overall loss of fitness of the individual and the population (Wolf et al., 2005). Polymorphisms are

also supported by a spatial, asynchronous version of the Devil's Compromise lifecycle, a scenario defined by individual cells moving asynchronously among spatially distinct environments. The contrast between the synchronous (selecting for *RPV*) and asynchronous (supporting non-phase varying polymorphisms) versions of the Devil's Compromise shows that stationary populations experiencing temporal environmental fluctuations face difficulties comparable to those experienced by mobile populations in spatially heterogeneous environments only if migration has a synchronous component, and underscores that it is selection over the *population*, as generated by a *time-varying environment* acting on cells with defective or absent environmental sensors, that selects for phase varying phenotype expression. Time-invariant, density-independent environments, and spatial, asynchronous selection over individual cells do not suffice.

We developed these results on a linear random matrix model because it captures essential features of the systems under investigation, and because a large body of analytical, simulation and conceptual machinery backs such models. The strength of this type of model is that (1) cells can have different phenotypic states at different times, (2) the advantage conferred by each state depends on the state of the environment, (3) cells can take in information from the environment to select a cell state, and (4) these sensors can be noisy, delayed, or misleading. However, the model does not explicitly capture resource competition and consumption. Though the approach we take is standard for investigating time-varying environments, and can be interpreted as competition for fluctuating resources, work demonstrating important effects of resource competition opens the question of what insights might be missed by not explicitly modeling population effects on the environment. Hansen and Hubbel, for example, demonstrated the competitive advantage of bacterial strains that can persist at low concentrations of a limiting resource (Hansen and Hubbel, 1980). In models such as ours resource competition would turn up indirectly as non-linear, saturating growth rates (Caswell, 2001, Chapter 16) or as additional environmental states and possibly non-Markovian environmental transitions (Tuljapurkar, 1990). In the case of simple saturating growth we can easily extend our model and show that our results qualitatively hold (though over slightly different parameter ranges). While we have not yet analysed models with non-Markov environments or continuous resource consumption for conditions giving rise to diversification strategies, this is clearly an important and rich area of study. By explicitly taking resource limitation and population effects on the environment into account, we expect to find even more situations in which diversification is the *ESS*. There is some evidence in the current literature, for example, that phenotypic

diversification of populations into fast and slow growers protects against fluctuations in nutrient levels (Balaban et al., 2004).

4.1. Competing hypotheses?

The results from this paper and from (Wolf et al., 2004), summarized in Table 3, add several variables to those proposed by Ancel-Meyers and Bull to predict selection among the different classes of adaptive phenotypic variation (Ancel Meyers and Bull, 2003). Specifically, we add (1) the (in)ability of a cell to sense its environment, representing defects in environmental transition observability, environmental identification accuracy, additive noise, and signal transduction delays, (2) the environmental rate of change (autocorrelation) matrixed with environmental lifecycle asymmetries, (3) frequency dependent selection in the environment (Wolf et al., 2005), and (4) cell state switching transition costs. Our results also provide a framework for considering competing hypotheses on the genesis of *RPV*, including (H1) *RPV* as a generator of antigenic diversity and immune system evasion, (H2) *RPV* as a means for searching receptor spaces, and (H3) *RPV* as a vehicle for seeding new environments with high fitness phenotypes then subject to clonal expansion on (Hallet, 2001).

Hypotheses (H1-3) on the genesis and utility of *RPV* are not contradictory. The combined forces exerted by a time-varying and frequency-dependent immune response conspire to select for *RPV* as a survival strategy in mammalian pathogens, though in this case the 'selected' cell state is 'immune naiveté'. Within a single host, time-varying selection is at work as the immune system cycles through the process of identifying antigens and producing antibodies (on the order of 4–7 days) (De Clercq, 2001), and as the population moves from host compartment to compartment over the course of an infection. Variability among potential hosts also creates time varying selection on slow scales, as populations move from host to host, and frequency-dependent selection. An antigenic variant is more likely to find a new host naïve of that variant if it is rare in the population, thus making the fitness conferred by any particular variant a function of its frequency in the population, a view supported by an analysis by Ancel-Meyers et al. of the role of phase shifting in *N. meningitides* pathogenicity (Meyers et al., 2003). Receptor variation is more likely to give rise to *RPV* among a smaller number of adhesin variants, acting as a form of memory for receptor distribution among and within hosts and the resulting time-varying and possibly frequency dependent selective forces acting on the population. All other things being equal, the fitness conferred by each type of adhesion molecule would be greatest when rare.

Table 3
Results summary^a

| Strategy | Sensor profile | | | | Environmental profile |
|-------------------------|-------------------------|----------------|----------|----------|---|
| | <i>O</i> | <i>A</i> | <i>D</i> | <i>N</i> | |
| RPV | No environmental sensor | | | | Devil's Compromise lifecycle: time-varying environment with different environmental states selecting for different cell states. Mild lifecycle asymmetries or large environmental autocorrelation. Optimal switching rates a function of lifecycle asymmetries and environmental autocorrelation. Time variation required (spatial variation insufficient). |
| | Low | X ^b | X | X | |
| | X | X | Long | X | Frequency dependent environment with mixed ESS. ESS = Polymorphism@ESS_f ; OPT = RPV_Opt. (modified Prisoner's Dilemma with RPV_Opt as the non-ESS cooperation strategy ²) |
| N.A. ^c | | | | | |
| Sensor based mixed | High | Poor | <Long | Low | Devil's Compromise lifecycle. Asymmetric lifecycle required. Optimal mixing probabilities biased toward selected cell-states in dominant environmental states. |
| Sensor based mixed; LPF | High | Poor | <Long | High | |
| Sensor based pure | High | High | <Long | X | Temporally or spatially varying environment with each environmental state selecting for a single cell state |
| Sensor based pure; LPF | High | Medium | <Long | Low | |
| | High | Medium | <Long | High | |
| Pure | No environmental sensor | | | | Devil's Compromise lifecycle. Lifecycle highly asymmetric without high environmental autocorrelation |
| | Low | X | X | X | |
| | X | X | Long | X | |

^aThis table summarizes how the *ESS* of a bacterial species depends on the environment(s) it lives in and the ability of cells to sense the environment. Strategies represented include *RPV* (randomly alternate between different phenotypes, with transition probabilities possibly a function of sensor information), sensor-based mixed (use sensor information to probabilistically diversify population upon transitioning to a new environment), sensor-based pure (use sensor information to deterministically select phenotype), low-pass filtered (LPF) versions of sensor-based mixed and pure strategies (deliberately build in response inertia to filter out sensor noise), and a sensor-independent pure strategy (monomorphic population in a single cell state). Sensor defects include unobservable environmental transitions (Observability (*O*) = Low), inability to accurately identify the identity of a new environment (Accuracy (*A*) = Low), long signal transduction delays relative to the frequency of environmental change (Delay (*D*) = Long), and high additive noise (Noise (*N*) = High). One reads the table as follows: “*RPV* is an *ESS* when the population lives in a Devil's Compromise time-varying environment and sensors are either absent or characterized by low observability of some environmental transitions or high signal transduction delays relative to the rate of environmental change”, and so on.

^bAn *x* in the table denotes ‘don't care’. ² Part II of this study (Wolf et al., 2005) describes how environments that select for rare phenotypes also select for diversification strategies, and define a modified Prisoner's Dilemma game with *RPV* at optimal rates serving as the non-*ESS* cooperation strategy.

^cResults from the analysis of frequency-dependent environments (Wolf et al., 2005) do not depend on sensor profile, unless one considers the possibility of cells communicating with one another in order to select the cooperation strategy of randomly phase variation at optimal (rather than *ESS*) rates.

Hypothesis (H3), that *RPV* provides a means for seeding new environments with high fitness phenotypes then subject to clonal expansion, is not really distinct from antigenic diversity and receptor space search hypotheses. Rather, it is an abstraction of the time-varying components of immune and receptor selectivity, and any other fluctuating environment that is the rule for microbial life. It is exactly the Devil's Compromise scenario described above, a time varying environment with different environmental states selecting for different cell states, with our added precondition that these environmental transitions be largely unobservable to the cell. *RPV* contains the memory of frequently visited environmental states, and, in its more mutation-like form, permits exploration and colonization of new niches, avoiding 'mutational error catastrophe' (Eigen, 2002) by confining high mutation rates to selected loci.

4.2. Name-that-game experiments

Though in this paper and in Wolf et al., 2005 we have constructed a framework for understanding some of the environmental and cell-sensory conditions that can give rise to *RPV* and other diversification strategies, experiments similar to those of Turner and Chao to reconstruct the RNA phage game (Turner and Chao, 1999, 2003) are needed to sift through hypotheses of how phase variation functions over the lifecycle of a particular organism (for caveats on experimentally validating game theoretic predictions, see (Orzack, 1994)). For example, with two environments $E1$ and $E2$, and two cell states x and y , the following experiments can 'name that game' or at least distinguish between Devil's compromise time-varying selection and frequency-dependent selection of the sort where the fitnesses of cell states are greatest when rare.

Phase variation as a Devil's compromise: If phase variation functions as a Devil's compromise, optimal or *ESS* within no single environment within the lifecycle yet required for long-term survival, experiments in which the population is locked in a single cell state and growth rate is measured in each environment would show that x does well in $E1$ and poorly in $E2$, and y does well in $E2$ and poorly in $E1$. The wild type phase varying population should grow in $E1$ and $E2$, though not as well as the selected pure strategists in each environment. Mixtures of phase-locked cells would see the x subpopulation out-competed by the y subpopulation in $E2$ and the y population out-competed by the x population in $E1$; cycling between $E1$ and $E2$ would lead to extinction or slowed growth of the entire polymorphic population relative to the phase varying population.

Diversification as a response to frequency-dependent selection: If phase variation or another diversification strategy is a response to frequency-dependent selection

in an environment Ei as described in Wolf et al. (2005), an experiment that mixes phase-locked x and y cells will show that the population settles to a steady-state composition, with neither x outcompeting y to extinction nor the other way around. Furthermore, a mixture of x and y cells will grow faster in Ei than does either a pure- x or a pure- y population. In the unlikely event that *RPV* is at optimal rates, playing the cooperation strategy in the game of modified Prisoner's Dilemma (see Wolf et al., 2005) rather than merely a single-genome means for generating the mixed *ESS* population composition, the addition of a few phase-locked x and y 'defector' cells to a wild type *RPV* population will result in a change in the steady-state population composition and a decrease of overall fitness of the population.

4.3. Do diverse designs play different games, or are they evolutionary spandrels?

Though in this paper we confine ourselves to the study of diversification strategies on the abstract phenotype, cell, and population levels, a more complete understanding calls upon us to focus 'down' a level of abstraction to study the similarities and differences among diversification mechanisms across pathways and species, and 'up' a level to define and compare the ecological composition of particular niches. The integration of analysis on all three levels in an evolutionary context is necessary if we hope to understand why some *RPV* mechanisms are based on DNA rearrangement, whereas others employ slipped strand mispairing (SSM), DNA shuffling by gene conversion and allele replacement, or epigenetic mechanisms, and the similarities and differences of network designs in each category (Henderson et al., 1999; Hallet, 2001). How much of the diversity in a population arises due to lack of control of noise in a system (endogenous or exogenous), and how much is there to serve an evolutionary purpose? Are these diverse designs merely evolutionary spandrels (Gould and Lewontin, 1979; Gould, 1997; Rao et al., 2004), or are differences in the physics of the environmental factors being sensed, the intracellular signaling molecules transducing environmental signals, pathway cross-regulation, or the 'game' of survival played by each microbe responsible for distinct mechanisms? To distinguish between these possibilities there is challenging theory and experiment to be done such as coming up with consistent theories of network evolution, experimentally measuring dynamics in single cells, tracking population heterogeneity under varying conditions, quantifying fitness, and designing experiments to test and generate game theoretic hypotheses. In any case, full elucidation of these themes will likely emerge from integrated application of classical molecular biology techniques with regulatory network deduction and analysis (Covert et al., 2004), comparative

genomics, cellular engineering (Kobayashi et al., 2004), and evolutionary game theory, an important addition to the Systems Biology toolbox (Kitano, 2002; Levchenko, 2003; Sauro et al., 2003) because of its power to relate the fitness of cellular design and behaviour to environmental and ecological dynamics (Wolf and Arkin, 2003).

5. Materials and methods

The results in this paper, even those that were subsequently generalized and proved rigorously, were initially observed by numerically exploring a family of models over a wide range of parameter values using the general purpose simulation and analysis software Matlab (Mathworks, Natick, Massachusetts, United States), as follows.

5.1. Periodically time varying environments (alternating between $N1$ time steps in $E1$ and $N2$ time steps in $E2$)

Simulation: A program to simulate population growth of imperfect-sensing cells living in a periodically varying environment calculates successive updates in the population vector \vec{X} in Eq. (1), alternating between $N1$ time steps in environment $E1$ (update \vec{X} using the matrix $R_{d1}T_{21}$ in the event of an environmental transition from $E2$ to $E1$ at the last time step; use R_{d1} otherwise) and $N2$ time steps in $E2$ (update \vec{X} using the matrix $R_{d2}T_{12}$ in the event of an environmental transition from $E1$ to $E2$ at the last time step; use R_{d2} otherwise).

Calculating the ESS: The ESS of cells with the sensor profile $Q = (p_{Obsij}, P_{Sij}, sq_{ij}(k))$; $i, j, k = 1 : 2$; growing in a periodically time-varying environment is determined by calculating the maximal eigenvalue of the 4×4 matrix $[T_{21}R_{d2}^{N2}T_{12}R_{d1}^{N1}]$ as a function of strategy $S = (sx_1, sy_1, sx_2, sy_2, P_1, P_2)$, for all strategies over the (digitized) strategy space $sx_1 = [0 : \Delta_s : s_{MAX}]$, $sy_1 = [0 : \Delta_s : s_{MAX}]$, $sx_2 = [0 : \Delta_s : s_{MAX}]$, $sy_2 = [0 : \Delta_s : s_{MAX}]$, $P_1 = [0 : \Delta_p : 1]$ and $P_2 = [0 : \Delta_p : 1]$. The upper bound s_{MAX} is chosen to be large enough to ensure that if any component of the fitness-maximizing ESS $S^* = (sx_1^*, sy_1^*, sx_2^*, sy_2^*, P_1^*, P_2^*)$ is finite, it is contained in the strategy search space. For the range of growth rates and lifecycles reported on in this paper, $s_{MAX} = 20$ is sufficiently large. Sampling increments Δ_s and Δ_p are initially chosen for a coarse-grained approximation to S^* (e.g. $\Delta_s = s_{MAX}/200$; $\Delta_p = 0.05$) and then reduced in the neighborhood of the approximation for arbitrarily greater accuracy. In the case of a symmetric environment and symmetric sensors (which produce a symmetric ESS), we simplified our search by setting $sx_2 = sy_1$ and $sy_2 = sx_1$. Table 1 summarizes the constraints on S^* indicating RPV, sensor-based mixed, sensor-based pure, and low-pass filtered versions of sensor-based mixed and pure strategies as an ESS. For

example, we conclude that the ESS is (1) RPV between cell states x and y if $(sx_1^* > 0, sy_1^* > 0, sx_2^* > 0, sy_2^* > 0, P_1^* = 1, P_2^* = 0)$; (2) a sensor-based mixed strategy if $(sx_1^* = 0, sy_1^* > 0, sx_2^* > 0, sy_2^* = 0, P_1^* < 1, P_2^* > 0)$, (3) a sensor-based pure strategy (not low pass filtered) if $(sx_1^* = 0, sy_1^* \rightarrow \infty, sx_2^* \rightarrow \infty, sy_2^* = 0, P_1^* = 1, P_2^* = 0)$; (4) a low-pass filtered sensor-based pure strategy if $(sx_1^* = 0, \infty > sy_1^* > 0, \infty > sx_2^* > 0, sy_2^* = 0, P_1^* = 1, P_2^* = 0)$; and so on. If the ESS is RPV, the optimal cell state switching transition rates are given by (sx_i^*, sy_i^*) . More exotic combinations, such as probabilistic mixing among RPV sub-strategies (e.g. $sx_1^* > 0, sy_1^* > 0, sx_2^* > 0, sy_2^* > 0, P_1^* < 1, P_2^* > 0$) or heterogeneous combinations of sub-strategies (e.g. $sx_1^* = 0, sy_1^* \rightarrow \infty, sx_2^* > 0, sy_2^* > 0, P_1^* = 1, P_2^* = 0$), are possible as well (data not shown).

Generating ESS bifurcation diagrams: To generate the ESS bifurcation diagrams in Fig. 10, we wrote a program that (1) calculates the ESS $S^* = (sx_1^*, sy_1^*, sx_2^*, sy_2^*, P_1^*, P_2^*)$ as a function of the two sensor parameters being varied over the entire strategy space, as described above, (2) generates an ESS function ‘ n ’ by assigning each point in the two dimensional sensor parameter space to one of five numbers: $n = 1$ if $S^* = RPV$; $n = 2$ if $S^* =$ sensor-based pure; $n = 3$ if $S^* =$ sensor-based mixed; $n = 4$ if $S^* =$ sensor-based pure, LPF; and $n = 5$ if $S^* =$ sensor-based mixed, LPF, and (3) generates the bifurcation diagram by applying the Matlab ‘contour’ plotting function to the ESS function ‘ n ’.

The no-sensor case is handled similarly, with the following simplifications: (1) a strategy is defined by the parameters $S = (sx, sy)$, (2) the fitness function is the maximal eigenvalue of the 2×2 matrix $[R_{d2}^{N2}R_{d1}^{N1}]$, and (3) Eq. (11) is simulated rather than Eq. (1).

5.2. Stochastically time-varying environments

Simulation: The program simulating population growth in a randomly time varying environment (1) invokes Eq. (5) to calculate the probability that the environment is in environmental state Ei at time $(k + 1)\Delta t$ given the environmental state at time $k\Delta t$, (2) selects the new environmental state with a random number generator, given this probability, (3) calculates the new population vector \vec{X} at time $(k + 1)\Delta t$ by multiplying the population vector at the previous step by the environmental-state-dependent rate and transition matrices as in Eq. (1) or (11). The initial environmental state is drawn from the stationary distribution over the environmental state space.

Calculating stochastic growth rate and growth rate variance: The simulation algorithm in Section 14.3.6.2 of Caswell (2001) by Cohen et al. (1983) is implemented to estimate $\log(\lambda_s)$, the stochastic growth rate or Lyapunov exponent of a population. The approximation

in Section 14.3.7 of Caswell (2001) is used to estimate the growth rate variance σ^2 .

Calculating the ESS: To calculate the ‘ESS’ of a population growing in a Markov environment, we followed the procedure described for periodic environments, with the exception that we used the stochastic growth rate $\log(\lambda_s)$ as a measure of fitness instead of a maximal eigenvalue of a matrix product. To investigate how an inclusion of growth rate variance in the fitness function would impact the ESS, we repeated this procedure with fitness functions $f_1 = \lambda \log(\lambda_s) - (1 - \lambda)\sigma^2$; $\lambda \in [0, 1]$, and $f_2 = \log(\lambda_s)/\sigma^2$.

5.3. Spatially heterogeneous environment with a Markov dispersal process governing individual cell movement from environment to environment

The program that determines the ESS of a strategy (sx, sy) of motile cells living in a spatially varying environment calculates the maximal eigenvalue of the matrix R_{ds} in Eq. (9) as a function of strategy (sx, sy) over the strategy space $sx = [0 : \Delta_s : s_{MAX}]$, $sy = [0 : \Delta_s : s_{MAX}]$, with $s_{MAX} > 20$. One could also consider population dispersal rates $m_{1,2}$ and $m_{2,1}$ as part of the strategy, and find the fitness-maximizing strategy $(sx^*, sy^*, m_{1,2}^*, m_{2,1}^*)$.

5.4. Parameter value ranges

Numerical experiments were run over the following parameter ranges (for $i, j = 1, 2$): *Environmental:* $1 \leq N1, N2 \leq 10,000$; $0 < p_{1,2}, p_{2,1} < 1$. *Growth:* $-4 \leq \lambda_x(i) - \mu_x(i) \leq 4$; $-4 \leq \lambda_y(i) - \mu_y(i) \leq 4$. *Strategies:* $0 \leq P_i \leq 1$; $0 \leq sx_i, sy_j \leq 20$. *Sensors:* $0 \leq p_{Obsji} \leq 1$; $0.5 \leq P_{Sij} \leq 1$; $0 \leq rate \leq 10$. *Dispersion:* $0 \leq m_{1,2} \leq 10$. *Discretization:* $0.0001 \leq \Delta t \leq 1$. Figs. 2–10 were generated with growth rates $\lambda_x(2) - \mu_x(2) = \lambda_y(1) - \mu_y(1) = -0.4$ and $\lambda_x(1) - \mu_x(1) = \lambda_y(2) - \mu_y(2) = 0.3$; $\Delta t = 1$. Other parameter values are specified in figure captions and text.

Contact dmwolf@lbl.gov for our Matlab m-files.

Acknowledgements

We thank Drs. Steve Orzack, David Steinsaltz, Wayne Getz, Daniel Portnoy, Christos Papadimitriou, Pat Flaherty and Sergei Plyasunov for helpful discussions and pointers to the literature. APA and DMW would like to acknowledge the Defense Advanced Research Project Agency, the Department of Energy and the Howard Hughes Medical Institute for support during the period of this project. VV would like to acknowledge the National Science Foundation for support.

Appendix A. Proofs

Proof of Theorem 1. The long-term growth rate of a pure strategy subpopulation in cell state s_i is governed by

$$\prod_{j=1}^m (g_{i,j})^{\tau_j}.$$

By the assumption made in the theorem, this product is < 1 for each cell state. Hence a population consisting of non phase-variable cells will go extinct with probability 1.

Next consider the random phase variable population P_2 . Assume that in each generation, a fraction, α , of bacteria in cell state S_i switch to cell state $S_{i'}$, for each pair i, i' of cell states, where

$$\alpha = \frac{\varepsilon}{(1 + 2\varepsilon)(k - 1)}.$$

Observe that this value of α satisfies

$$g_{\tau(j),j}(1 - (k - 1)\alpha) > 1 + \varepsilon$$

and hence while in environment E_j , the subpopulation in cell state $\tau(j)$ keeps growing even though a part of it is lost in each generation due to switching. Observe further that λ and α are related as follows: $\lambda = 2 \log(1/\alpha) / \log(1 + \varepsilon)$.

While in an environment E_j , we will only consider the subpopulation in the preferred cell state $\tau(j)$, and when the environment changes from E_j to $E_{j'}$, we will only consider the subpopulation that switches from cell state $\tau(j)$ to $\tau(j')$. Let Y_j be a random variable denoting the number of generations spent in environment E_j . In this part of the lifecycle, the total growth rate of this subpopulation is

$$\geq (g_{\tau(j),j}(1 - (k - 1)\alpha))^{Y_j} > (1 + \varepsilon)^{Y_j} \alpha.$$

Next, let us consider this subpopulation as it goes through n environments. Let Y_1, \dots, Y_n be random variables denoting the number of generations spent in these environments. The total growth rate in this part of the lifecycle is

$$\geq (1 + \varepsilon)^{Y_1 + Y_2 + \dots + Y_n} \alpha^n.$$

Let random variable $Y = Y_1 + Y_2 + \dots + Y_n$. We want to place an upper bound on the lower tail of Y . Let X_1, \dots, X_n be geometrically distributed random variables with $\Pr[X_i = t] = p(1 - p)^{t-1}$. Since the probability that M remains in any state is $\geq 1 - p$, Y_i dominates X_i , and placing an upper bound on the lower tail of X will help place an upper bound on the lower tail of Y . More precisely,

$$\Pr\left[Y < \frac{n(1 - \delta)}{p}\right] \leq \Pr\left[X < \frac{n(1 - \delta)}{p}\right].$$

Consider a coin having probability of p of coming up Heads. Observe that X_1 has the same distribution as the number of flips of this coin until the first Head, and X has the same distribution as the position of the n th Head. Clearly, $E[X_i] = 1/p$ and $E[X] = n/p$. We want to upper bound the probability of the event $[X < n(1-\delta)/p]$.

Let a new random variable X' be the number of Heads among the first $n(1-\delta)/p$ coin flips. Then the event $[X < n(1-\delta)/p]$ is the same as the event $[X' \geq n]$. The probability of the latter is easily upper bounded, since X' can be viewed as the sum of $n(1-\delta)/p$ independent Poisson trials with mean $\mu = n(1-\delta)$. Let $\Delta = \delta/(1-\delta)$, so that $(1+\Delta)\mu = n$. Applying the Chernoff bound (Alon, 2000), we get

$$\begin{aligned} Pr\left[X < \frac{n(1-\delta)}{p}\right] &= Pr[X' \geq (1+\Delta)\mu] \\ &< \exp -(\mu\Delta^2/4) \\ &= \exp -\left[\frac{n\delta^2}{4(1-\delta)}\right]. \end{aligned}$$

Therefore, the event $[Y \geq n(1-\delta)/p]$ has overwhelming probability. By the choice of p , $n(1-\delta)/p \geq n\lambda$. Therefore, with overwhelming probability, $Y_1 + Y_2 + \dots + Y_n \geq n\lambda$. Hence the total growth rate of the subpopulation is at least

$$(1+\varepsilon)^{n\lambda} \alpha^n = (1+\varepsilon)^{n\lambda} \left(\frac{\varepsilon}{(1+2\varepsilon)(k-1)}\right)^n \geq \frac{1}{\alpha^n}.$$

[Observe the role played by the relationship between λ and α in simplifying this expression.] Hence, the size of the random phase variable population P_2 diverges with n , with overwhelming probability. \square

Proof of Theorem 2. For each environment E_j , let $\sigma(j)$ denote the unique strategy that has the largest growth rate. By the assumption in Theorem 1, the growth rate of this strategy is $> 1 + 2\varepsilon$. Consider the sensor-based mixing population P_3 as it goes through n environmental states, say E_1, \dots, E_n , and assume that

$$R_s = \begin{bmatrix} \lambda_x(1) - \mu(1)_x - m_{1,2} - sx & sy & m_{2,1} & 0 \\ sx & \lambda_y(1) - \mu(1)_y - m_{1,2} - sy & 0 & m_{2,1} \\ m_{1,2} & 0 & \lambda_x(2) - \mu(2)_x - m_{2,1} - sx & sy \\ 0 & m_{1,2} & sx & \lambda_y(2) - \mu(2)_y - m_{2,1} - sy \end{bmatrix}. \quad (10)$$

Y_1, \dots, Y_n are random variables denoting the number of generations spent in these environments. The dominant term in the growth rate of P_3 is obtained by tracing in each environment the subpopulation having

the largest growth rate, and is given by

$$\prod_{j=1}^n (1 - (k-1)\alpha)(g_{\sigma(j),j})^{Y_j}.$$

The corresponding term for the random phase variable population P_2 differs in two respects: First, this (preferred) subpopulation depletes by a fraction $(k-1)\alpha$ in each generation due to switching to other strategies. Second, a corresponding fraction of other subpopulations switches to this (preferred) subpopulation. However, since the other subpopulations have lower growth rates, the first effect dominates the second and results in a net depletion. Hence the growth rate of P_3 dominates that of P_2 . \square

Appendix B. (Model of asynchronous, spatial Devil's Compromise)

In the asynchronous, spatial version of the Devil's Compromise scenario, individual cells move asynchronously from spatially discrete environment to environment according to a Markov process, rather than having the entire population subject to a time-varying environment that transitions between environmental states in a Markov fashion, as does Eq. (1). A bacterial population consisting of cells without environmental sensors that can alternate between x and y states and move asynchronously between environments E_1 and E_2 follows a trajectory given by Eq. (9), defined by a state vector \vec{Y} and rate matrix R_{ds} , defined below:

$$\vec{Y}_{k+1} = R_{ds} \vec{Y}_k. \quad (9)$$

The population state vector $\vec{Y} = [x_1, y_1, x_2, y_2]'$, where x_i is the number of cells in the population in state x in environment E_i ($i = 1$ or 2), and y_i is the number of cells in the population in state y in environment E_i . The rate matrix $R_{ds} = e^{R_s \Delta t}$ is the discretized version of the continuous-time growth rate matrix R_s (shown below), derived from the rate equations for the Master Equation tracking $\mathbf{Pr}(\vec{Y} = [nmr q]')$:

In matrix R_s , $\lambda_i(i)$ and $\mu_j(i)$ are the birth and death transition probability rates, respectively, of cells in state j (x or y) in environment E_i , sx and sy the x -to- y and y -to- x cell state transition probability rates, respectively,

and m_{ij} the transition state probabilities of individual cells moving from environment E_i to E_j . Note that in contrast to Eqs. (1) and (11), Eq. (9) has a time-invariant rate matrix (R_{ds} does not depend upon the time step k).

Appendix C. (Reduced model for the no-sensor case)

Without sensors, Eq. (1) reduces to the two dimensional system:

$$\vec{X}_{k+1} = R'_{di}(k)\vec{X}_k. \quad (11)$$

The population state vector $\vec{X} = [x \ y]'$, where x is the number of cells in the population in state x and y is the number of cells in the population in state y with sensors reading $\vec{E} = E_i$. As in Eq. (1), the rate matrix $R'_{di} = e^{R_i \Delta t}$ is the discretized version of the continuous-time growth rate matrix R'_i (shown below), derived from the rate equations for the Master Equation tracking $\Pr([x \ y]) = [n \ m]$ in environment E_i , where n and m are nonnegative integers:

$$R'_i = \begin{bmatrix} \lambda_x(i) - \mu_x(i) - sx & sy \\ sx & \lambda_y(i) - \mu_y(i) - sy \end{bmatrix}. \quad (12)$$

In the matrix R'_i , $\lambda_s(i)$ and $\mu_s(i)$ are the birth and death transition probability rates, respectively, of cells in state s ($s = x$ or y) in environment E_i ($i = 1$ or 2), and parameters sx and sy are transition probability rates of switching from cell state x -to- y or y -to- x , respectively. Otherwise, modelling and simulation proceed as described in Section 5.

Appendix D. (Generalizing the Microbial Diversification Game (MDG) model)

The model instantiated as Eq. (1) can be extended to capture an arbitrary number of cellular and environmental states, cell state switching costs, microbe-environment interactions such as nutrient consumption and the creation of waste products, ecological diversity, and intercellular communication, among other realistic complexities. For example, with n cellular and m environmental states, the population state vector is the $nm \times 1$ column vector $X = [x_{11}, x_{21}, \dots, x_{n1}, \dots, x_{1m}, x_{2m}, \dots, x_{nm}]'$, where x_{ij} = number of cells in cell state s_i with sensor reading E_j . Rate matrices R_i are expanded accordingly to be of size $nm \times nm$, with $n \times n$ block matrices along the diagonal representing Markov chain, sensor-based sub-strategies S_i over the n cell states, and off-diagonal blocks consisting of $n \times n$ diagonal sensor switching matrices. Cell state switching costs can be explicitly represented by doubling the size of the cell state space, adding low growth rate or high resource

consumption ‘refractory’ sub-states that the cell must pass through upon switching to each new cell state. Ecological diversity is easily represented as well, by equations with a population column vector of length $n_1 m_1 \times n_2 m_2 \dots \times n_k m_k$, where k is the number of different microbial species, n_j and m_j are the number of possible cellular and environmental states, respectively, of species j : a vector consisting of ‘stacked’ population vectors of each species, with growth rates that can depend upon total cross-species population size and composition to explicitly represent inter- and intra-strain competition. Resource competition can be indirectly represented as nonlinear, saturating growth rates (Caswell, 2001, Chapter 16) or as additional environmental states corresponding to different nutrient levels, and possibly non-Markovian environmental transitions (Tuljapurkar, 1990). Explicit, continuous representation of resource consumption and competition can be achieved by adding resource variables to the model’s state space as in Hansen and Hubbel (1980).

References

- Abraham, J.M., Freitag, C.S., Clements, J.R., Eisenstein, B.I., 1985. An invertible element of DNA controls phase variation of type 1 fimbriae of *E. coli*. Proc. Natl Acad. Sci. USA 82 (17), 5724–5727.
- Alon, N.A., Spencer, J., 2000. The Probabilistic Method. Wiley, New York.
- Ancel Meyers, M., Bull, J.J., 2003. Fighting change with change, adaptive variation in an uncertain world. Trends Ecol. Evol. 17 (12), 551–557.
- Balaban, N.Q., Merrin, J., Chait, R., Kowalik, L., Leibler, S., 2004. Bacterial persistence as a phenotypic switch. Science 305 (5690), 1622–1625.
- Blomfield, I.C., 2001. The regulation of pap and type 1 fimbriation in *E. coli*. Adv. Microb. Physiol. 45, 1–49.
- Boynifield, H.R., Hughes, K.T., 2003. Flagellar phase variation in *Salmonella enterica* is mediated by a posttranscriptional control mechanism. J. Bacteriol. 185 (12), 3567–3574.
- Boyd, S., Barratt, C., 1991. Linear Controller Design: Limits of Performance. Prentice-Hall, Englewood Cliffs, NJ.
- Caswell, H., 2001. Matrix population models: construction, analysis, and interpretation. Sinauer Associates Inc., Sunderland, MA.
- Cohen, J.E., Christensen, S.W., Goodyear, C.P., 1983. A stochastic age-structured population model of striped bass (*Morone saxatilis*) in the Potomac River. Can. J. Fish. Aquat. Sci. 40, 2170–2183.
- Comins, H.N., Hamilton, W.D., May, R.M., 1980. Evolutionarily stable dispersal strategies. J. Theor. Biol. 82 (2), 205–230.
- Cooper, V.S., Lenski, R.E., 2000. The population genetics of ecological specialization in evolving *E. coli* populations. Nature 407 (6805), 736–739.
- Coote, J.G., 2001. Environmental sensing mechanisms in *Bordetella*. Adv. Microb. Physiol. 44, 141–181.
- Covert, M.W., Knight, E.M., Reed, J.L., Herrgard, M.J., Palsson, B.O., 2004. Integrating high-throughput and computational data elucidates bacterial networks. Nature 429 (6987), 92–96.
- De Clercq, E.D.A. (Ed.), 2001. Antiretroviral Therapy. ASM Press, Washington, DC.
- Doebeli, M., 1995. Updating Gillespie with controlled chaos. Am. Nat. 146 (3), 479–487.
- Dybvig, K., Sitaraman, R., French, C.T., 1998. A family of phase-variable restriction enzymes with differing specificities generated by

- high-frequency gene rearrangements. *Proc. Natl Acad. Sci. USA* 95 (23), 13923–13928.
- Eigen, M., 2002. Error catastrophe and antiviral strategy. *Proc. Natl Acad. Sci. USA* 99 (21), 13374–13376.
- Ferrell Jr., J.E., 2002. Self-perpetuating states in signal transduction: positive feedback, double-negative feedback and bistability. *Curr. Opin. Cell Biol.* 14 (2), 140–148.
- Fussenegger, M., Rudel, T., Barten, R., Ryll, R., Meyer, T.F., 1997. Transformation competence and type-4 pilus biogenesis in *Neisseria gonorrhoeae*—a review. *Gene* 192 (1), 125–134.
- Gally, D.L., Bogan, J.A., Eisenstein, B.I., Blomfield, I.C., 1993. Environmental regulation of the fim switch controlling type 1 fimbrial phase variation in *E. coli* K-12: effects of temperature and media. *J. Bacteriol.* 175 (19), 6186–6193.
- Gillespie, J.H., 1973. Natural selection with varying selection coefficients—a haploid model. *Genet. Res.* 21, 115–120.
- Gillespie, J.H., 1975. The role of migration in the genetic structure of populations in temporarily and spatially varying environments I. Conditions for polymorphism. *Am. Nat.* 109 (966).
- Gillespie, D.T., 1992. Markov processes: an introduction for physical scientists. Academic Press, Inc., London.
- Gonzalez-Pastor, J.E., Hobbs, E.C., Losick, R., 2003. Cannibalism by sporulating bacteria. *Science* 301 (5632), 510–513.
- Gould, S.J., 1997. The exaptive excellence of spandrels as a term and prototype. *Proc. Natl Acad. Sci. USA* 94 (20), 10750–10755.
- Gould, S.J., Lewontin, R.C., 1979. The spandrels of San Marco and the Panglossian paradigm: a critique of the adaptationist programme. *Proc. R. Soc. Lond. B Biol. Sci.* 205 (1161), 581–598.
- Grimshaw, C.E., Huang, S., Hanstein, C.G., Strauch, M.A., Burbulis, D., et al., 1998. Synergistic kinetic interactions between components of the phosphorelay controlling sporulation in *Bacillus subtilis*. *Biochemistry* 37 (5), 1365–1375.
- Grossman, A.D., 1995. Genetic networks controlling the initiation of sporulation and the development of genetic competence in *Bacillus subtilis*. *Annu. Rev. Genet.* 29, 477–508.
- Hallet, B., 2001. Playing Dr Jekyll and Mr Hyde: combined mechanisms of phase variation in bacteria. *Curr. Opin. Microbiol.* 4 (5), 570–581.
- Hansen, S.R., Hubbel, S.P., 1980. Single-nutrient microbial competition: qualitative agreement between experimental and theoretically forecast outcomes. *Science* 207 (4438), 1491–1493.
- Harmer, G.P., Abbott, D., Taylor, P.G., Parrondo, J.M., 2001. Brownian ratchets and Parrondo's games. *Chaos* 11 (3), 705–714.
- Hauck, C.R., Meyer, T.F., 2003. Small talk: Opa proteins as mediators of *Neisseria*-host-cell communication. *Curr. Opin. Microbiol.* 6 (1), 43–49.
- Hecker, M., Volker, U., 2001. General stress response of *Bacillus subtilis* and other bacteria. *Adv. Microb. Physiol.* 44, 35–91.
- Henderson, I.R., Owen, P., Nataro, J.P., 1999. Molecular switches—the ON and OFF of bacterial phase variation. *Mol. Microbiol.* 33 (5), 919–932.
- Hernday, A., Krabbe, M., Braaten, B., Low, D., 2002. Self-perpetuating epigenetic pili switches in bacteria. *Proc. Natl Acad. Sci. USA* 99 (Suppl. 4), 16470–16476.
- Howell-Adams, B., Seifert, H.S., 2000. Molecular models accounting for the gene conversion reactions mediating gonococcal pilin antigenic variation. *Mol. Microbiol.* 37 (5), 1146–1158.
- Kishony, R., Leibler, S., 2003. Environmental stresses can alleviate the average deleterious effect of mutations. *J. Biol.* 2 (2), 14.
- Kitano, H., 2002. Computational systems biology. *Nature* 420 (6912), 206–210.
- Kobayashi, H., Kaern, M., Araki, M., Chung, K., Gardner, T.S., et al., 2004. Programmable cells: interfacing natural and engineered gene networks. *Proc. Natl Acad. Sci. USA*.
- Lachmann, M., Jablonka, E., 1996. The inheritance of phenotypes: an adaptation to fluctuating environments. *J. Theor. Biol.* 181 (1), 1–9.
- Lande, R., Orzack, S.H., 1988. Extinction dynamics of age-structured populations in a fluctuating environment. *Proc. Natl Acad. Sci. USA* 85 (19), 7418–7421.
- Levchenko, A., 2003. Dynamical and integrative cell signaling: challenges for the new biology. *Biotechnol. Bioeng.* 84 (7), 773–782.
- Mangan, S., Alon, U., 2003. Structure and function of the feed-forward loop network motif. *Proc. Natl Acad. Sci. USA* 100 (21), 11980–11985.
- Martinez de Tejada, G., Cotter, P.A., Heining, U., Camilli, A., Akerley, B.J., et al., 1998. Neither the Bvg-phase nor the vrg6 locus of *Bordetella pertussis* is required for respiratory infection in mice. *Infect. Immun.* 66 (6), 2762–2768.
- Maynard Smith, J., 1982. *Evolution and the Theory of Games*, Cambridge University Press.
- Maynard Smith, J.P.G.R., 1973. The logic of animal conflict. *Nature* 246 (5427), 15–18.
- McAdams, H.H., Arkin, A., 1997. Stochastic mechanisms in gene expression. *Proc. Natl Acad. Sci. USA* 94 (3), 814–819.
- McClure, W.R., 1980. Rate-limiting steps in RNA chain initiation. *Proc. Natl Acad. Sci. USA* 77 (10), 5634–5638.
- Merton, R.C., 1982. On the microeconomic theory of investment under uncertainty. In: Arrow, K.J., Intriligator, M.D. (Eds.), *Handbook of Mathematical Economics*. North-Holland, Amsterdam.
- Meyers, L.A., Levin, B.R., Richardson, A.R., Stojiljkovic, I., 2003. Epidemiology, hypermutation, within-host evolution and the virulence of *Neisseria meningitidis*. *Proc. R. Soc. Lond. B Biol. Sci.* 270 (1525), 1667–1677.
- Mittler, J.E., 1996. Evolution of the genetic switch in temperate bacteriophage. I. Basic theory. *J. Theor. Biol.* 179 (2), 161–172.
- Moran, A.P., Prendergast, M.M., 2001. Molecular mimicry in *Campylobacter jejuni* and *Helicobacter pylori* lipopolysaccharides: contribution of gastrointestinal infections to autoimmunity. *J. Autoimmun.* 16 (3), 241–256.
- Moses, E.K., Good, R.T., Sinistaj, M., Billington, S.J., Langford, C.J., et al., 1995. A multiple site-specific DNA-inversion model for the control of Omp1 phase and antigenic variation in *Dichelobacter nodosus*. *Mol. Microbiol.* 17 (1), 183–196.
- Msadek, T., 1999. When the going gets tough: survival strategies and environmental signaling networks in *Bacillus subtilis*. *Trends Microbiol.* 7 (5), 201–207.
- Oppenheim, A.V., Wilsky, A.S., Young, I.T., 1983. *Signals and Systems*. Prentice-Hall, Englewood Cliffs, NJ.
- Orzack, S.H., Sober, E., 1994. Optimality models and the test of adaptationism. *Am. Nat.* 143 (3), 361–380.
- Power, P.M., Roddam, L.F., Rutter, K., Fitzpatrick, S.Z., Srikhanta, Y.N., et al., 2003. Genetic characterization of pilin glycosylation and phase variation in *Neisseria meningitidis*. *Mol. Microbiol.* 49 (3), 833–847.
- Rao, C.V., Wolf, D.M., Arkin, A.P., 2002. Control, exploitation and tolerance of intracellular noise. *Nature* 420 (6912), 231–237.
- Rao, C.V., Kirby, J.R., Arkin, A.P., 2004. Design and diversity in bacterial chemotaxis: a comparative study of *E. coli* and *Bacillus subtilis*. *PLoS Biol.*
- Samoilov, M., Arkin, A., Ross, J., 2002. Signal processing by simple chemical systems. *J. Phys. Chem. A* 106 (43), 10205–10221.
- Satake, A., Sasaki, A., Iwasa, Y., 2001. Variable timing of reproduction in unpredictable environments: adaptation of flood plain plants. *Theor. Popul. Biol.* 60 (1), 1–15.
- Saunders, N.J., Moxon, E.R., Gravenor, M.B., 2003. Mutation rates: estimating phase variation rates when fitness differences are present and their impact on population structure. *Microbiology* 149 (Pt. 2), 485–495.

- Sauro, H.M., Hucka, M., Finney, A., Wellock, C., Bolouri, H., et al., 2003. Next generation simulation tools: the Systems Biology Workbench and BioSPICE integration. *Omics* 7 (4), 355–372.
- Steinmoen, H., Knutsen, E., Havarstein, L.S., 2002. Induction of natural competence in *Streptococcus pneumoniae* triggers lysis and DNA release from a subfraction of the cell population. *Proc. Natl Acad. Sci. USA* 99 (11), 7681–7686.
- Stewart, R.C., Van Bruggen, R., 2004. Association and dissociation kinetics for CheY interacting with the P2 domain of CheA. *J. Mol. Biol.* 336 (1), 287–301.
- Stibitz, S., Aaronson, W., Monack, D., Falkow, S., 1989. Phase variation in *Bordetella pertussis* by frameshift mutation in a gene for a novel two-component system. *Nature* 338 (6212), 266–269.
- Stumpf, M.P., Laidlaw, Z., Jansen, V.A., 2002. Herpes viruses hedge their bets. *Proc. Natl Acad. Sci. USA* 99 (23), 15234–15237.
- Sumby, P., Smith, M.C., 2003. Phase variation in the phage growth limitation system of *Streptomyces coelicolor* A3(2). *J. Bacteriol.* 185 (15), 4558–4563.
- Tuljapurkar, S., 1982. Population dynamics in variable environments. *Theor. Popul. Biol.* 21, 141–165.
- Tuljapurkar, S., 1990. In: Levin, S. (Ed.), *Population Dynamics in Variable Environments*. Springer, Berlin.
- Turner, P.E., Chao, L., 1999. Prisoner's dilemma in an RNA virus. *Nature* 398 (6726), 441–443.
- Turner, P.E., Chao, L., 2003. Escape from Prisoner's Dilemma in RNA phage phi6. *Am. Nat.* 161 (3), 497–505.
- Vidyasagar, M., 1992. *Nonlinear Systems Analysis*. Prentice-Hall, Engelwood Cliffs, NJ.
- Webb, J.S., Givskov, M., Kjelleberg, S., 2003. Bacterial biofilms: prokaryotic adventures in multicellularity. *Curr. Opin. Microbiol.* 6 (6), 578–585.
- Weiss, A.A., Falkow, S., 1984. Genetic analysis of phase change in *Bordetella pertussis*. *Infect. Immun.* 43 (1), 263–269.
- Wolf, D.M., Arkin, A.P., 2002. Fifteen minutes of fim: control of type 1 pili expression in *E. coli*. *Omics* 6 (1), 91–114.
- Wolf, D.M., Arkin, A.P., 2003. Motifs, modules and games in bacteria. *Curr. Opin. Microbiol.* 6 (2), 125–134.
- Wolf, D.M., Vaziran, V.V., Arkin, A.P., 2005. A microbial modified Prisoner's Dilemma game: how frequency-dependent selection can lead to random phase variation. *J. Theor. Biol.*, this issue.